

# **Visual Feedback from the Own Acting Hand Modulates the Activity of Grasping Neurons in Monkey Premotor Area F5**

Caselli L<sup>1</sup>, Oliynyk A<sup>1</sup>, Gesierich B<sup>1,2</sup>, Craighero L<sup>1</sup>, Fadiga L<sup>1,3</sup>

(1) University of Ferrara, Dept. Biomedical Sciences, Ferrara (IT)

(2) University of Trento, Center for Mind/Brain Sciences, Rovereto (IT);

(3) The Italian Institute of Technology, Genova (IT)

## **ABSTRACT**

Visual responses in the monkey ventral premotor cortex have been explored since long time. Area F5 has been shown to contain grasping neurons that visually discharge either to 3D-object presentation (canonical neurons) or to the observation of actions performed by other individuals (mirror neurons). It has been suggested that the mirror response results from the progressive generalization to others' actions of a visuomotor link which, during action execution, associates the vision of the own acting effector with the motor program selected for the ongoing action. To start tackling this hypothesis, we specifically asked whether area F5 contains neurons responding to the observation of one's own grasping movement. A specially-designed experimental apparatus was used to test F5 neuronal discharge while monkeys were engaged in a reach-to-grasp task and either continuous or transient visual information on the ongoing movement was made available. Single-unit activity was additionally recorded from the hand region of the primary motor cortex (area F1). Neuronal responses evoked by the vision of the own entire grasping action or of brief meaningful phases of it were detected in both areas. However, F5 modulation was overall more strong and specific. The finding that neurons in area F5 exhibit discharge properties that are common to both purely motor and mirror neurons allows the formulation of important assumptions about the critical role of online visual information during grasping and the nature of the mirror discharge.

## INTRODUCTION

Visual responses in the premotor cortex have been extensively studied in the last two decades. Thereby, ventral premotor area F5, residing in the posterior bank and convexity of the inferior arcuate sulcus (iAS), has turned out to be particularly important for the visuomotor transformations it carries out in the domain of visually-guided grasping movements (Rizzolatti et al. 1988; Murata et al. 1997; Raos et al. 2006). Grasping is one of the most evolved types of primate behavior, resulting from a complex visuomotor process that transforms the object's three-dimensional structure into specific motor commands to select the optimal finger configuration for grasping. During pre-shaping, fingers progressively open and straighten up to reach a point of maximum grip aperture, which is followed by closure of the grip with gradual finger flexion as the hand approaches the object (Jeannerod et al. 1995).

Intracortical microstimulation and single-unit recordings in the macaque monkey have demonstrated that grasping relies on a fronto-parietal visuomotor circuit including, besides area F5, the inferior intraparietal area AIP (Murata et al. 1996; Murata et al. 2000), the ventro-rostral part of area F2 in the dorsal premotor cortex (Raos et al. 2004) and the primary motor cortex F1 (Dum and Strick 2005; Umiltà et al. 2007). Successful execution of grasping much depends on the integrity of area F1, which directly controls finger muscles and is known to be crucial for skilled hand function. Lesions or inactivation of this area produce a severe deficit of individual finger movements and, consequently, of normal grasping (Liu and Rouiller 1999; Fogassi et al. 2001). F5, which represents, through cortico-cortical connections, one of the major inputs to the hand field of area F1 (Matelli et al. 1986), is the motor region most critically involved in pre-configuring the hand according to the visual properties of the object. After inactivation of area F5, hand shaping is markedly impaired, with fingers position not properly matching the size and shape of the object, thus causing grasping failure (Fogassi et al. 2001).

In addition to purely motor grasping neurons, specifying types of hand shaping (e.g., precision or whole-hand grip), or timing the action discharging during different grasping phases, two main categories of F5 visuomotor neurons have been described so far. On the basis of their visual properties they have been named *canonical* and *mirror* visuomotor neurons.

*Canonical* neurons, mainly located on the posterior bank of the iAS (F5ab sector), display a 3D object-related visual selectivity that is almost congruent with the grip-specificity of their motor discharge. Area F5ab represents the main target of projections originating from area AIP, which, in turn, has been shown to contain three main classes of neurons (Taira et al. 1990; Murata et al. 2000;

Sakata et al. 1995), all of them contributing to the visuomotor transformation from object description to hand shaping selection. AIP *visual-dominant* neurons respond during object presentation and grasping only when full visual information on the movement is available (they do not discharge when grasping is performed in dark); *motor-dominant* neurons are active during grasping, independently of whether the movement is visible or not, and do not fire during object observation; *visual-motor* neurons are similar to the visual-dominant ones but they also respond during grasping in dark, though the discharge is much weaker than that displayed in full light. This latter neuronal class resembles that represented by F5 canonical neurons, suggesting that the motor activity observed in AIP may reflect a corollary discharge initiating in F5ab and maintained through a F5-AIP reverberating circuit, active during the whole grasping period (Taira et al. 1990).

It is worth mentioning that in the study by Murata et al. (2000) a particular class of AIP visuomotor neurons, devoid of any object-related visual selectivity but exhibiting a grasping motor response that was stronger in light than in dark, was additionally described. These *nonobject-type* neurons, whose discharge properties can be considered as intermediate between the motor-dominant and the visual-motor classes, have been thought to respond to handgrip selectivity or, more importantly for the purposes of the present work, to a combined view of handgrip and object. Indeed, although contradictory arm/hand kinematics results have been reported about the effects of removing online vision on the control of reach-to-grasp movements (Winges et al. 2003; Rand et al. 2007), visual feedback signals are of unquestionable importance in goal-directed hand movements, especially for the formation of finger grip during prehension (Jeannerod et al. 1995; Jeannerod 1986). An alternative account for the functional properties of these *nonobject-type* AIP neurons is that they might reflect mirror-neuron-like characteristics (see below).

*Mirror* neurons, mainly sited on the F5 cortical convexity (F5c), are visually triggered by the observation of a biological agent performing a given goal-directed action (e.g. grasping), typically *mirroring* the motor response normally recorded from the same neurons during the actual execution of a similar action (di Pellegrino et al. 1992; Rizzolatti et al. 1996; Gallese et al. 1996). The matching between the observed and the executed action encoded by a single mirror neuron response has been shown to encompass different levels of congruence, ranging from a very strict to a broader visuomotor correspondence. For example, neurons whose motor discharge is selective for a precision grip can either only respond to the observation of actions involving the same precision grip or can be visually triggered by any type of hand grasping. Broadly congruent mirror neurons are of particular interest since they generalize the goal of the observed action over many instances of it. A recent fMRI study performed on monkeys (Nelissen et al. 2005) demonstrated that the

ventral premotor cortex hosts at least two main distinct representations of others' actions. Besides area F5c, which was found to be active only when the observed acting person was in full view, hence displaying a highly specific context-related action representation, the anterior sector of area F5 (area F5a), located in the depth of the iAS, appeared to encode actions in a more abstract way: visual stimuli such as mimicked actions, the view of the only grasping hand or actions performed by a robotic arm were all as effective as an acting human being in triggering F5a activation.

The existence of mirror neurons in area F5 that generalize the goal of a specific observed action to many other examples of it, thus suggesting the association of different visual information to a common goal-related motor-invariant signal, and the fact that these cells are part of a neuronal circuit, additionally including the PF/PFG complex in the inferior parietal lobule (Petrides and Pandya 1984; Matelli et al. 1986; Fogassi et al. 2005; Fogassi and Luppino 2005) and the superior temporal sulcus (STS) (Perrett et al. 1989), which describes actions also in purely visual terms, have led to the formulation of a sensory feedback-based theory accounting for the generation of mirror neurons (Rizzolatti and Fadiga 1998). According to this theory, the mirror discharge develops from the observation of one's own acting effector, seen from slightly different perspectives, performing repetitively the same action. Through the visual feedback system normally guiding action execution, motor invariance is extracted from the different visual perspectives, thus initially creating a matching between the action and the vision, by the agent performing the action, of his/her own ongoing movement. Once this visuomotor link is established, it will then be progressively generalized to the observation of actions executed by other individuals. Very recent results, achieved by applying this model to an acting artificial system, showed that this could be the case (Metta et al. 2006; Craighero et al. 2007).

At present, there is no evidence in favour of the existence, in area F5, of neurons showing visuomotor responses that couple the execution with the observation of one's own actions. The presence of such neurons is a necessary prerequisite to demonstrate the validity of the sensory feedback-based theory mentioned above.

The aim of the present study was to start clarifying this issue. As a first step along this direction, we specifically investigated the presence, in area F5, of neurons similar to the non-object visually-responsive neurons previously described in area AIP (Murata et al. 2000), whose grasping-related activity is significantly strengthened when the monkey observes its own hand action (i.e., under full light conditions), with respect to a condition during which it cannot (i.e., in darkness). These discharge properties, which could be considered as transitional to those of purely motor and mirror neurons, would represent a conceivable neuronal indicator of the visuomotor matching

proposed by the aforementioned theory. However, such a modulation could also be the neuronal counterpart of the efficacy of the online visual information in properly guiding the hand during object grasping. Therefore, to better identify neurons showing activity specifically evoked by the observation of the own grasping action, we explored the influence on the F5 single-neuron responses of very brief motor-relevant visual feedbacks (i.e., light flashes delivered at precise instants during critical grasping phases) that do not modify arm/hand kinematics, though providing the system with strategically useful visual information. As a control, the activity of neurons in the hand representation of area F1 was recorded as well.

## METHODS

### *Surgery*

Single-unit activity was recorded from both ventral premotor area F5 and primary motor cortex F1 in three hemispheres (contralateral to the moving forelimb) of two awake behaving monkeys (*Macaca fascicularis*). The monkeys (one female and one male, respectively weighing 5.7 kg and 4.9 kg and referred as to MK1 and MK2) were specifically trained to perform a behavioral task (see following text), while seating on a primate chair. After training, a recording chamber and head-restraint device were surgically implanted. All experimental protocols were approved by the Veterinarian Animal Care and Use Committee of the University of Ferrara, by the Italian Ministry of Health and complied with the European laws on the use of laboratory animals.

Structural CT and MRI images were respectively used in MK1 and MK2 to stereotactically place the recording chamber over the cortical region including the posterior bank of the inferior arcuate sulcus and central sulcus, where areas F5 and F1 are located. In MK1, the cortical surface was indirectly rendered after Computer Assisted Tomography (CAT) acquisition, through reversal of inner skull surface, and 3D-reconstructed by using ETDIPS (NIH, NUS, <http://www.cc.nih.gov/cip/software/etdips/>) and Rhinoceros<sup>®</sup> 2.0 (Robert McNeel & Associates, USA) softwares. The coordinate system of the obtained 3D-images of the brain was then adjusted to the standard stereotaxic coordinates system based on the orbitomeatal plane and with a custom-designed software (Virtax, <http://web.unife.it/progetti/neurolab/>, Gesierich et al., in preparation) we determined the position of the target cortices by using as references both the sulcal pattern impressed on the internal surface of the skull and the stereotaxic atlas by Szabo and Cowan (Szabo and Cowan 1984). The inferior surface of the titanium recording chamber cylinders (height 20 mm, inner  $\varnothing$  24 mm, out  $\varnothing$  30 mm) was virtually modeled through Rhinoceros<sup>®</sup> 2.0 software, so to perfectly fit the skull curvature of the monkeys, maximizing adhesion between the implant and the bone. The chamber models were then manufactured by a MAXNC 15 computer-driven 3D milling machine (MAXNC inc., Arizona, U.S.A.) by using the MillWizard software (Delcam Artcam, U.K.).

All surgical implantations were carried out under aseptic procedures and general anesthesia. Monkeys were pre-medicated with atropine sulfate (0.1 mg/Kg, IM, MONICO S.p.A., Italy) and tiletamine-zolazepam (20 mg/Kg, IM, Zoletil, VIRBAC, S.A., France), and anesthetized by isoflurane (Abbott S.p.A., Illinois, U.S.A.) for the whole duration of surgery. Antibiotics and analgesics were administered postoperatively and experiments were started at least two weeks after the surgery.

### *Electrophysiology*

Single-unit recordings were performed by using varnish-insulated tungsten microelectrodes with impedance 0.15–1.5M $\Omega$  (measured at 1 kHz). Electrodes were obtained repetitively passing the tip of tungsten rods ( $\varnothing$  250  $\mu$ m, A-M Systems, inc. WA, U.S.A.) through a KOH (10% in distilled water) etching solution by means of a metal electrode etcher (BAK Electronics, inc., MD, U.S.A.), and covering them with multiple layers of varnish (SIVAMID 595/38M, ELANTAS Electrical Insulation, Germany) that were oven-dried at high temperature (400°C). This procedure has the advantage of providing microelectrodes with the desired tip and highly resistant insulation.

During each experimental session, the microelectrode was inserted perpendicular to the cortical surface (i.e., with an angle of 32–40° with respect to sagittal plane) and was slowly advanced through the cortex by means of a hydraulic microdrive (Kopf Instruments, CA, U.S.A.; step resolution, 10  $\mu$ m). The recorded signal was amplified  $\times 10000$  (BAK Electronics, Germantown MD, USA), filtered by a dual variable filter (VBF-8, KEMO Ltd., Backenham, UK) (300–5000 Hz bandwidth), digitized (PCI-6071E, National Instruments, USA) at a sampling rate of 10 kHz and stored for further off-line analysis. Action potentials were on-line discriminated by a dual voltage-time window discriminator (BAK Electronics, Germantown MD, USA) and fed to an Audio monitor (Grass Instruments, USA) to give the experimenter an auditory feedback on the neuron discharge during testing. Data analysis was performed after off-line discrimination of single-units from multi-spike recordings carried out by means of a custom-made LabView-based software (Olyinik et al., in preparation).

The recording microelectrodes were also used for intracortical microstimulation (ICMS, train duration, 50–100 ms; pulse duration, 0.2 ms; frequency, 330 Hz; current intensity, 3–40  $\mu$ A). The current strength was controlled on an oscilloscope by measuring the voltage drop across a 10k $\Omega$  resistor in series with the stimulating electrode.

### *Recording sites*

The chamber rostro-caudal and medio-lateral axis dimension was such as to allow to record from a brain region spanning area F1, the whole ventral premotor cortex and the caudal part of the Frontal Eye Fields (FEF). The ventral part of the agranular frontal cortex was functionally explored through single unit recordings and ICMS to assess the location of areas F1, F4 and F5. Criteria and functional characteristics described by Umiltà et al. (2001) were used to distinguish motor and premotor areas as well as regions within area F5 characterized by a high density of neurons exhibiting hand-related activity during goal-directed actions.

### *Naturalistic testing*

Naturalistic testing was used to select neurons to be then thoroughly examined through the experimental paradigm. Single-neuron activity was studied with reference to the execution of different hand/arm movements, selected to elicit different grip types or to the application of different sensory stimuli, according to procedures described in other previous studies (Rizzolatti et al. 1990; Rizzolatti et al. 1988; Gallese et al. 1996). For example, the presentation of a small piece of food placed inside a slot required the monkey to perform a precision grip, by opposing the first phalanx of the thumb to the first phalanx of the index finger, while a syringe filled with juice evoked a power grip, with the fingers wrapped around the object and the palm in contact with it. Visual canonical properties were tested by presenting the monkey with 3D objects of different size, shape and orientation. Visual mirror properties were tested by performing a series of hand actions (grasping holding, manipulating) in front of the monkey. This functional characterization, together with the ICMS data, allowed us to select hand-related neurons predominantly selective for precision grasping. Particular attention was paid so to discard cells showing canonical or mirror visual properties and include just those showing motor discharge only.

### *Behavioral apparatus and paradigm*

The pre-selected grasping neurons were studied by means of a behavioral apparatus specifically designed to make the animals perform a reach-to-grasp task, which naturally implied the execution of a precision grip to open the door of a container and get a piece of food which was hidden inside (Fig. 1A). The container was mounted on a vertical rack at reaching distance (approximately 30 cm) in front of the primate chair, so that, in case, the monkeys were forced to watch their own grasping trajectory. The precision grip had to be performed on a small plastic cube (0.8 x 0.8 x 0.8 mm) embedded in a groove, serving as the door handle (Fig. 1B). To ensure that the movement was accurately executed even under dark conditions, the cube was translucent and dimly back-illuminated by a red LED. The LED intensity was kept very low and did not allow the vision of the approaching hand. Each trial started with the monkey's right (or left) hand positioned close to the body, on the hip board of the primate chair. An external sliding door, overlying the target door for the animal, was opened at distance by the experimenter, giving the monkey a go-signal to start the reach-to-grasp movement (Fig. 1C). As the monkey touched the handle correctly, with both the thumb and index fingers, a TTL signal was sent via an electronic circuit to the acquisition PC to synchronize the neuronal data. Data included one second before and two seconds after handle grasping were stored for each trial.

The task was performed under four different conditions:

- 1) *Light (L)* condition: grasping was executed with continuous vision of the own hand movement (i.e., in full light).
- 2) *Dark (D)* condition: grasping was executed in absence of any visual information on the own movement (i.e., in darkness).
- 3) *Pre-touch (PT) flash* condition: grasping was executed in dark with instantaneous visual feedback before touching, during the handgrip shaping phase. The scene was briefly illuminated by a 20  $\mu$ s xenon light flash triggered by the signal of the hand crossing an infrared barrier built by a pyroelectric sensor located 10 cm in front of the food container.
- 4) *Touch (T) flash* condition: grasping was executed in dark with instantaneous visual feedback at hand-object contact. The scene was briefly illuminated by a 20  $\mu$ s xenon light flash delivered as both the thumb and index finger touched the target handle.

Experimental conditions were presented in blocks of twelve trials and administered with the above temporal order in all sessions. The *Light* condition was repeated at the end of each recording session just to confirm the stability of neuronal activity (*Light 2* condition).

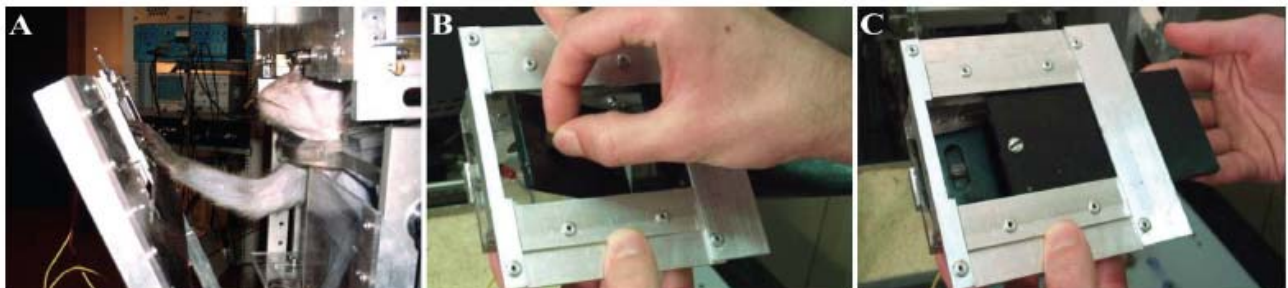


**Figure 1.** Experimental setup. A: Lateral view of the behavioral apparatus, requiring the monkey to perform a reach-to-grasp task. B: Demonstration of the precision grip the monkey had to execute in order to open the door of the food container. C: The target door was covered by an outer sliding door that the experimenter opened at each trial onset, giving the monkey a go-signal to start moving the hand from the resting position.

### *Hand kinematics acquisition*

In a preliminary session, the behavioral task was administered to MK1 and kinematics of the arm/hand was recorded to ensure that it was comparable in the different grasping conditions, including *Light 2* condition. Markers were placed on the wrist of the monkey's hand to evaluate the transport component of the movement and on the last phalanx of the thumb and index finger to measure grip aperture during hand shaping. The markers were fixated on plastic strings, adjustable in length, that were tightened around the wrist and relevant fingers. After a first brief period of familiarization with the markers, the monkey was able to execute the experimental task naturally.

Twelve kinematics recordings were collected for each experimental condition. The three-dimensional trajectories of each marker were acquired (240 frames/sec) by an infrared-sensitive motion tracking system (ProReflex/Qualisys Track Manager, Qualisys AB, Sweden). The same signal used for triggering the neuronal data acquisition (hand-handle contact) was also acquired to temporally align kinematics recordings.

### *Spike sorting*

The isolation of single neurons from multispikes recordings was performed off-line by using Singular Value Decomposition of the data matrix containing the different spike waveforms, followed by Fuzzy C-mean clustering analysis of Principal Components in the multi-dimensional space (Oliynyk et al., in preparation). The good quality of the discrimination was confirmed by evaluating the single-unit interspike interval histograms and the main quantitative parameters of cluster quality, including  $L_{ratio}$  measures (Lewicki 1998; Schmitzer-Torbert et al. 2005; Bezdek et al. 1984). A custom-made software was created for this purpose and all implemented algorithms were entirely realized by LabVIEW 7.0 software (National Instruments, U.S.A.). A part of the DataEngine V.i library (MIT GmbH, Germany) for LabVIEW was used for the programming and implementation of the spike sorting algorithm.

## ***Analysis***

### *Kinematics analysis*

The 3D position over time of the wrist, thumb and index finger markers was off-line reconstructed by using a position prediction algorithm provided by Qualisys Track Manager software (Qualisys AB, Sweden) and the following kinematic parameters of interest were extracted for each condition: maximal wrist velocity, maximal grip aperture, deceleration time, defined as the interval between the time of wrist peak velocity and handle touch instant, and aperture-closure time, defined as the interval between the time of maximal grip aperture and handle touch instant. A non-parametric one-way ANOVA (*Kruskal-Wallis test*, 5% alpha level) was performed to compare *Light*, *Dark*, *PT flash*, *T flash* and *Light 2* conditions for each of these parameters.

### *Single-neuron analyses*

To ensure that the motor response of the selected neurons was related to hand grasping and thus was modulated by the task, the difference in activity between a baseline epoch (*epoch 1*) and a movement-related epoch (*epoch 2*) was statistically assessed in all conditions for each neuron by means of a two-way repeated-measure analysis of variance (ANOVA, 5% alpha level) with *epoch*

(*epoch 1* and *epoch 2*) and *condition* (*D*, *L*, *PT flash* and *T flash*) as factors. *Epoch 1* corresponded to a pre-movement period, during which the hand was about to initiate the movement from the starting position (first 500 ms in the trial); *epoch 2* corresponded to a 500-ms grasping-related period including both the hand shaping and finger closure phases, going from 250 ms before the instant at which the hand touched the target handle (*pre-touch* sub-epoch) to 250 ms after it (*post-touch* sub-epoch).

Neurons which did not show any significant difference in firing rates between *epoch 1* and *epoch 2* in any condition (i.e., conjunct lack of *epoch* main effect and of significant differences between epochs for one particular condition, as resulting from the *Tukey's Least Significant Difference* (LSD) post-hoc tests performed on significant *epoch x condition* interactions) were discarded from further analyses. To assess whether the activity of the neurons was modulated by the vision of the acting hand, data analyses were first focused on detecting differences in activity between *D* and *L* conditions in *epoch 2* (significant *epoch x condition* interactions, with *D* different from *L* condition in *epoch 2* at the LSD post-hoc tests). In order to better appreciate even subtle effects on the single-neuron activity, a two-tail paired *Student's t-test* (5% alpha level) comparing *D* vs. *L* mean firing rates was additionally performed on a 100-ms bin, which was stepped through the trial by 20-ms increments. Figure 5D shows the output of this analysis performed on the *D* and *L*-related activity of two single cells taken from the F5 and F1 recorded samples (Fig. 5C). A neuron was considered as significantly modulated if it displayed a statistically significant difference in activity between the two conditions in at least two consecutive time bins. According to the direction of the effect shown in the *pre-* and *post-touch* sub-epochs of *epoch 2*, each neuron was then classified as positively or negatively modulated by light in both or either of the two sub-epochs.

To investigate the effect of the light flashes on grasping-related neuronal activity, a similar approach was employed. In view of the fact that *PT flash* and *T flash* were transient visual manipulations and represented hybrid situations with respect to the *D* and *L* conditions as for both physical and functional aspects, direct comparisons between activity during flashes and *D* (or *L*) were avoided at the first-level analysis. This choice was also driven by the purpose of getting rid of any unspecific arousal-related flash effect. Thus, as a first step, the above described running *t-test* analysis was used to contrast single-neuron discharge in *PT flash* and *T flash* conditions, with the aim to primarily identify neurons firing preferentially when a light flash was delivered at a specific relevant instant in the trial. In particular, we were interested in any firing difference observed between the two flash conditions within *epoch 2*, with the idea that, even a very short-lived visual information, if relevant for the ongoing hand movement, should modulate the grasping-related activity of the neuron. Once flash-selective neurons, if any, were detected, their flash-related

activity was then compared with the activity they exhibited in the *D* and *L* condition and thoroughly studied at the population level.

*Estimation of neuronal response latency and peak.* Response latency was calculated using a version of the time to half-height of the peak nonparametric technique (Gawne et al. 1996), which detects the midpoint between the minimum and maximum values of the single-neuron firing rate histogram, smoothed with the optimal bandwidth. We chose to implement this technique because it gives a latency measure which is less susceptible to noise than the one obtained through other methods computing latency at the onset of the neuronal response, when the rate of change in activity is quite low and therefore characterized by an unfavorable signal-to-noise ratio. By definition, the maximum firing value in the histogram is the peak of neuronal discharge. The single-neuron spike train, averaged and aligned with respect to the handle touch instant (time 0) for each condition, was convolved with a smooth Gaussian kernel function with window width set to 20 ms, to obtain a spike density function (SDF) providing a continuous and fine (1-ms binned) time-dependent measure of the firing pattern. The first time this SDF exceeded the average of the minimum and peak values in the period including the grasping movement (first 1250 ms in the trial) was regarded as the estimated response latency of the neuron in one given experimental condition.

### *Population analyses*

Normalization was achieved for each neuron composing a population through ms-by-ms dividing the smoothed SDF relative to one given experimental condition by the highest discharge value (peak of activity) observed across all four conditions. Population plots were obtained by simply averaging the normalized smoothed SDF of the included neurons.

Statistical analyses on latency or peak firing rates were performed assigning to each entry in a given pre-selected population, the normalized activity values respectively corresponding to the time of half-maximum or maximum activity (see above) for each single unit.

Weighted average (*WA*) latency and peak firing rates of one single neuron in a group were computed according to the following formula:

$$WA_n = (\sum_i x_i * f_i) / \sum_i f_i$$

where  $x_i$  is the discharge of the neuron  $n$  at the latency (or peak) time of each neuron  $i$  in the group and  $f_i$  is the latency (or peak) time of each neuron  $i$  in the group.

Analyses on the activity recorded within a specific trial period (e.g., *epoch 2*) during one particular condition were carried out on the single-neuron mean raw firing rates in the target period, normalized to the maximum activity across all four conditions, as just described.

*Estimation of neuronal latency of light- and flash-selectivity.* The same method used for computing single-neuron motor response latency was employed to calculate the neuronal latency of light and flash selectivity expressed at the population level. In this case, latency was defined as the time at which firing in *L* vs. *D* (or in *PT flash* vs. *T flash*) trials differed from one another in a relevant way. Therefore, we compared the time at which the difference in the population activity between the two conditions under investigation reached half of the maximum value, considering the normalized mean firing rate differences computed on a sliding 100-ms bin (sliding step, 20 ms). This method was used to have an additional measure for expressing the latency of neuronal selectivity, besides the one given by the running *t-test* analysis (see above), returning the time course of the selectivity of the neuronal population.

*Estimation of magnitude of light- and flash-selectivity.* The strength of light- and flash-selectivity was evaluated by using a Receiver Operating Characteristic (ROC) analysis (Metz 1978), which measures the degree of overlap between two response distributions. Hence, given for instance the two distributions of neuronal activity *L* (i.e., Light-related) and *D* (i.e., Dark-related), for each observed single-neuron firing rate, the proportion of *L* against the proportion of *D* response distribution exceeding that firing rate was plotted and the area under the plotted curve (ROC area) was computed, yielding a single value for that comparison. This method has several advantages. First, it provides an assumption-free estimate of the degree of overlap between *L* and *D* distributions: values near 0.5 indicate large overlap between the distributions, whereas values close to 0 or 1 indicate small or no overlap, with every value drawn from one distribution exceeded by the other entire distribution and vice versa. Second, it can be conveniently interpreted as the performance of an ideal observer in a two-way forced choice task. Third, it is independent of the firing rate of the neuron and can thus be used to compare the activity of neurons with widely different baseline and dynamic firing rates.

Population ROC area values, comparing *L* vs. *D* (or *PT flash* vs. *T flash*) distributions, were either computed every 20-ms step in a 100-ms bin covering all the trial period, or averaged within selected grasping epochs.

## RESULTS

### *Kinematics results*

Arm/hand kinematics parameters acquired from MK1 were analyzed. Figure 2B shows the temporal trajectories of wrist velocity and grip size for each of the five conditions considered: *L*, *D*, *PT flash*, *T flash* and *L2*.

Statistical analysis (*Kruskal-Wallis test*, 5% alpha level) on the transport component of the movement revealed that the maximal wrist velocity was significantly higher during the *Light* conditions (*L* and *L2*) than during *PT flash* ( $P < 0.02$ ) and *T flash* ( $t = 12.7$ ,  $P < 0.05$ ) conditions (Fig. 2A, *Maximal velocity* plot). Accordingly, a significant faster deceleration time was observed in full light (*L* and *L2*) with respect to all dark conditions, including *D*, *PT flash* and *T flash* ( $P < 0.0001$ ) (Fig. 2A, *Deceleration time* plot). Importantly, maximal wrist velocity and arm deceleration phase were not different in the two flash conditions and in the dark.

As far as the grip parameters are concerned, maximal grip aperture was considerably greater in the dark and flash conditions than in the light, especially if considering differences with the *L2* condition ( $P < 0.03$ ) (Fig. 2A, *Maximal grip aperture* plot). This specific result may be explained in terms of a rebound effect: after repetitively grasping in the dark over the previous three consecutive blocks of trials (in which *D*, *PT flash* and *T flash* conditions were administered), in the *L2* condition the monkey assumed a peak grip size even less large than the one adopted in the first *L* condition. Conversely, the wider finger aperture observed under dark conditions suggests that, in absence of any visual information, the monkey was enlarging the grip size safety margin to increase the chances of successfully grasping the door handle. To this purpose, after maximal aperture was reached, fingers also closed more slowly in the dark and flash conditions than in the light ( $P < 0.02$ ) (Fig. 2A, *Aperture-closure time* plot). Again, there was no significant difference among the dark and flash conditions, in neither grasping parameter.

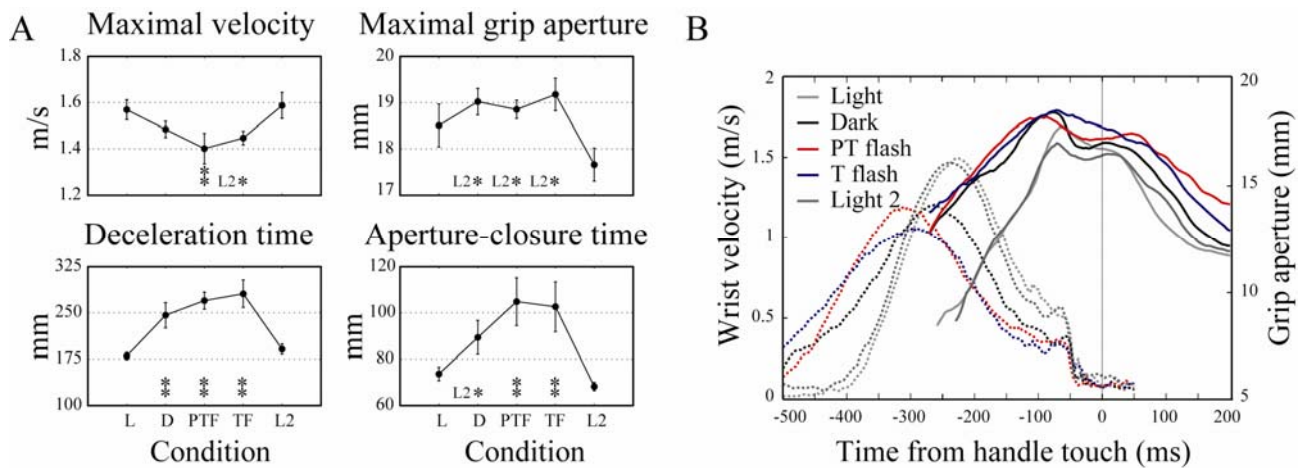


**Figure 2.** A: Average kinematic parameters (maximal velocity, maximal grip aperture, deceleration time, aperture-closure time) recorded for each condition during the behavioral experiment conducted with MK1. Deceleration and aperture closure times are respectively measured as the intervals from the time of maximal velocity and from the time of maximal grip aperture to handle touch instant. B: Wrist velocity (dashed lines) and grip aperture (solid lines) recorded over time for each condition (*Light 2* condition is also included). Asterisks within each plot represent significant differences (*Kruskal-Wallis test*, 5% alpha level) of D, PT flash or T flash condition with respect to either or both light conditions.

Overall, these findings confirm the results of previous kinematics studies on humans, reporting an increase in the duration of wrist deceleration and fingers closure phases when visual feedback was entirely or partially blocked during movement (Jackson et al. 1995; Schettino et al. 2003; Wings et al. 2003) or when vision of the own hand was prevented (Gentilucci et al. 1994; Churchill et al. 2000; Schettino et al. 2003; Rand et al. 2007). Also the adoption of a wider maximal grip aperture in absence of any visual feedback (Jakobson and Goodale 1991; Jackson et al. 1995) or without vision of the hand (Churchill et al. 2000) has been already previously observed.

Notably, the fact that no substantial kinematics dissimilarity was found between the two flash conditions (both resembling the dark condition) suggests that the present behavioral task represented a valuable tool to explore the effect of the vision of the own acting hand on the response of grasping neurons in cortical motor areas, without necessarily invoking kinematics variables.

#### *Microstimulation data*

We performed 149 penetrations in the three hemispheres of the two monkeys (see Table 1). The respective functional maps are illustrated in Figure 3 (A, B, C). Figure 3D displays the three-

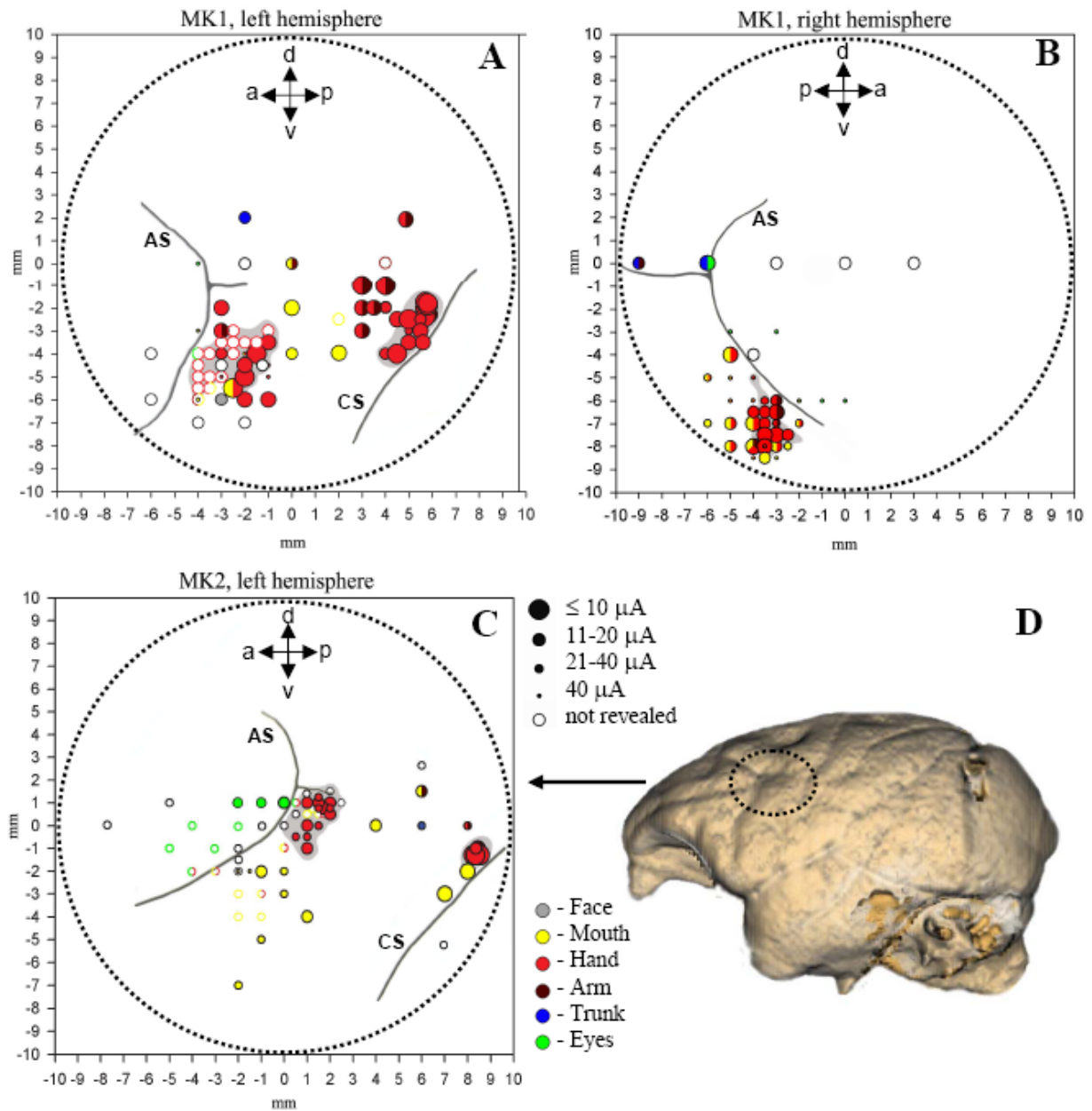


**Figure 3.** Penetration sites. A, B: Surface location of the electrode penetrations in both hemispheres of MK1. C: Penetrations in the left hemisphere of MK2. (D) Lateral view of the brain surface reconstruction of MK2. Encircled region shows the position of the recording chamber. Filled symbols indicate sites where intracortical microstimulation (ICMS) elicited hand movements at different current intensity thresholds. The size of the circles is correlated with the value of the lowest threshold found in each penetration, as indicated in the key of the figure. Unfilled symbols indicate sites not tested with ICMS. Each color refers to the specific body part controlled by the neurons encountered in each penetration. AS, arcuate sulcus; CS, central sulcus. Grey regions highlight penetrations where neurons were recorded while the monkeys were performing the reach-to-grasp task.

dimensional reconstruction of the brain surface of MK2 that was used to position the recording chamber on the skull. Penetrations are marked according to the specific body-part movements associated with the neuronal responses and the current intensity threshold at which those

movements were evoked through ICMS. As threshold, we defined the minimal current intensity at which visually detectable movements were evoked in 50% of stimulation trials.

All sites in the rostral bank of the central sulcus (area F1) were excitable with low-threshold currents (MK1,  $9.8 \pm 0.8 \mu\text{A}$ ; MK2,  $11.4 \pm 2.2 \mu\text{A}$ , mean  $\pm$  S.E.M.) evoking hand or finger movements. Microstimulation of the penetration sites rostral to F1 hand representation (estimated to be located in area F4) evoked face and axial movements at higher thresholds (MK1,  $21.1 \pm 5.9 \mu\text{A}$ ; MK2,  $27.9 \pm 3.2 \mu\text{A}$ ). Neurons in this region appeared to show large somatosensory receptive fields on the face and body and visual receptive fields in register with the somatosensory ones. The hand representation in area F5 was identified further rostrally, in the posterior bank of the iAS, on the basis of distal movements evoked by stimulation at the following thresholds: MK1,  $24.2 \pm 2.8 \mu\text{A}$ ; MK2,  $28.2 \pm 2.3 \mu\text{A}$ . The discharge of the neurons in this region was often related to goal-directed actions, mainly including grasping. The presence of microstimulation-induced eye movements (current intensity thresholds: MK1,  $25.9 \pm 4.6$ ; MK2,  $24.2 \pm 5.7$ ) and the recording of saccade-related activity in a region anterior to area F5 and to the iAS, were considered as functional markers of the FEF.

Grey regions highlight penetrations where grasping motor neurons were recorded while the monkeys were engaged in performing the behavioral task. Overall, the grasping-related activity of the neuronal samples recorded from the three monkey hemispheres during the task was congruent with the functional characterization obtained through ICMS and naturalistic testing.

### *Neurons database*

A total number of 295 and 236 grasping motor neurons were respectively isolated from F5 and F1 areas of MK1 and MK2 during 271 recording sessions. Of these neurons, 169 of area F5 and 129 of area F1 survived the selection criteria (stability of the recording throughout the duration of the task and sufficient number of trials recorded per each condition). One F1 neuron was subsequently discarded since, as revealed by the two-way *epoch x condition* ANOVA, its activity during grasping was not significantly different from that displayed during the pre-movement period. Therefore, the database for the present study consisted of 169 F5 neurons (102 recorded from the two hemispheres of MK1 and 67 recorded from the left hemisphere of MK2) and 128 F1 neurons (106 and 22 recorded from the left hemispheres of MK1 and MK2, respectively). Details concerning all recording sessions are reported in Table 1.

**Table 1.** Summary of the database.

	<i>Monkey 1</i>				<i>Monkey 2</i>			
	F5		F1		F5		F1	
	LH	RH	LH	RH	LH	RH	LH	RH
	Right hand	Left hand	Right hand		Right hand		Right hand	
Penetrations	41	32	21	--	45	--	10	--
Recording sessions	52	62	67	--	67	--	23	--
Isolated units	67	116	204	--	112	--	32	--
Analyzed database								
<i>S</i> : session	S = 23	S = 32	S = 67		S = 49		S = 17	
<i>N</i> : neurons	N = 38	N = 64	N = 106	--	N = 67	--	N = 22	--
PT flash delivery (median (IQR))*	-169 ms (-225/-107)	-200 ms (-242/-133)	-126 ms (-178/-93)	--	-215 ms (-252/-167)	--	-190 ms (-251/-135)	--

\* Median and inter-quartile range (IQR) of times of *PT flash* delivery, according to the instant when the hand (right or left, depending on the recorded hemisphere) crossed the IR barrier before touching the door handle (temporal values are aligned to handle touch).

#### *Dark vs. light conditions: types of neuronal modulations*

By looking at the results of the 2-way ANOVA, post-hoc tests performed on significant *epoch x condition* interactions revealed that *within epoch 2* 14% of F5 neurons and 9% of F1 neurons showed higher activity during *L* than *D* condition, while 19% (F5) and 23% (F1) of neurons exhibited the opposite modulation. The amount of F5 and F1 neurons which did not fire differently in the two conditions (non-modulated neurons) was comparable (67% and 68%, respectively).

The running *t-test* comparing *D* vs. *L* activity throughout *epoch 2* confirmed this pattern of results, though revealing a larger amount of effects due to the less restricted significance criteria of the analysis (see *Methods*). According to the period in which the neuronal modulation was observed, neurons were classified as showing one particular effect (*L>D* or *D>L*) in the *pre-touch* sub-epoch, in the *post-touch* sub-epoch, at the instant when the hand touched the handle, or through whole *epoch 2* (Tab. 2; Fig. 4). The number of modulated neurons was comparable in the two areas (61% in F5 and 54% in F1); more precisely, the portions of F5 neurons strengthening (22%) or diminishing (39%) their activity due to full vision of the ongoing movement, mostly reflected those of F1 (22% and 32%, respectively). However, and more interestingly, in both areas, the majority of *L*-sensitive effects were clustered in the *pre-touch* sub-epoch (14% in F5 and 13% in F1), while the opposite modulations principally emerged in the *post-touch* sub-epoch (22% in F5 and 20% in F1).

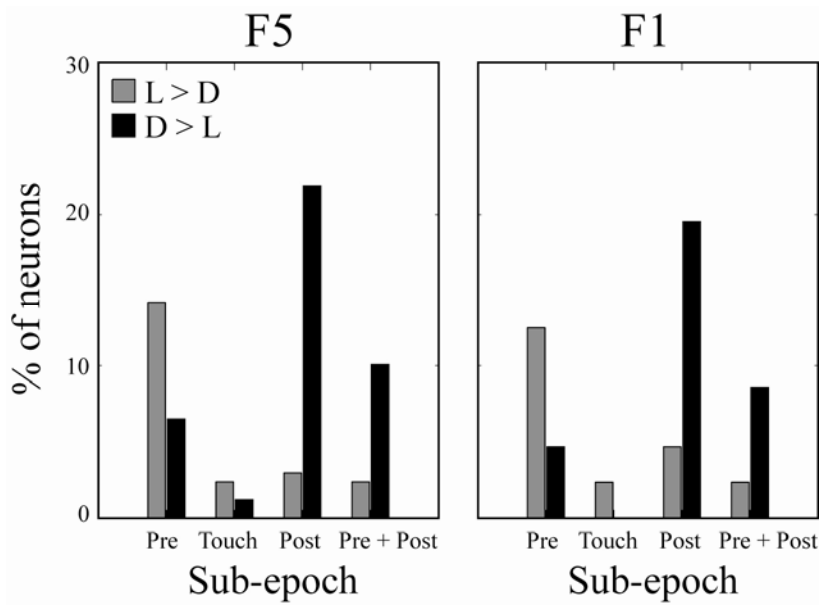


**Figure 4.** Distribution of F5 and F1 neurons with  $L/D$  modulation across the different grasping-related sub-epochs, as summarized in table 1.

**Table 2.** Summary of results from the running paired *t*-test analysis comparing single-neuron activity in *L* vs. *D* condition in a 100-ms bin shifted through the trial by 20 ms steps.

	<i>Pre-touch</i> (-250 ms – 0 ms)		<i>Touch</i> (around 0 ms)		<i>Post-touch</i> (0 ms - 250 ms)		<i>Pre- +</i> <i>Post-touch</i>		<i>Sub-total</i>	
	MK1	MK2	MK1	MK2	MK1	MK2	MK1	MK2	MK1	MK2
<b>F5</b>										
<i>L</i> > <i>D</i>	13	11	3	1	5	--	4	--	25	13
	24 (14%)		4 (2%)		5 (3%)		4 (2%)		37 (22%)	
<i>D</i> > <i>L</i>	4	7	1	1	23	14	10	7	35	32
	11 (7%)		2 (1%)		37 (22%)		17 (10%)		67 (39%)	
Modulated	35		6		42		21		104 (61%)	
<i>Spurious</i>									20	10
									30 (18%)	
<i>L</i> = <i>D</i>									22	13
									35 (21%)	
<b>Total</b>									<b>169 (100%)</b>	
<b>F1</b>										
<i>L</i> > <i>D</i>	13	3	3	--	6	--	3	--	25	3
	16 (13%)		3 (2%)		6 (5%)		3 (2%)		28 (22%)	
<i>D</i> > <i>L</i>	4	2	--	--	21	4	10	1	35	7
	6 (5%)		--		25 (20%)		11 (9%)		42 (32%)	
Modulated	22		3		31		14		70 (54%)	
<i>Spurious</i>									28	6
									34 (27%)	
<i>L</i> = <i>D</i>									18	6
									24 (19%)	
<b>Total</b>									<b>128 (100%)</b>	

Neurons are divided according to the monkey from which they were recorded (MK1 or MK2) and the specific sub-epoch within *epoch 2* (going from 250 ms before to 250 ms after handle touch) in which they showed the *D/L* modulation. The entry “*Spurious*” indicates neurons showing opposite *D/L* modulations within *epoch 2*. The percentage values always refer to the entire sample of recorded neurons.

Figures 5 and 6 show single-neuron examples of the most significant neuronal categories just described. Spike density plots and respective rasters are aligned to the instant at which the hand touched the door handle and describe the single-unit activity during the whole grasping period (first 1500 ms in the trial). For descriptive purposes, plots in Figure 6C also include the subsequent food-grasping neuronal response, not examined in the current work. The most relevant effects of light on

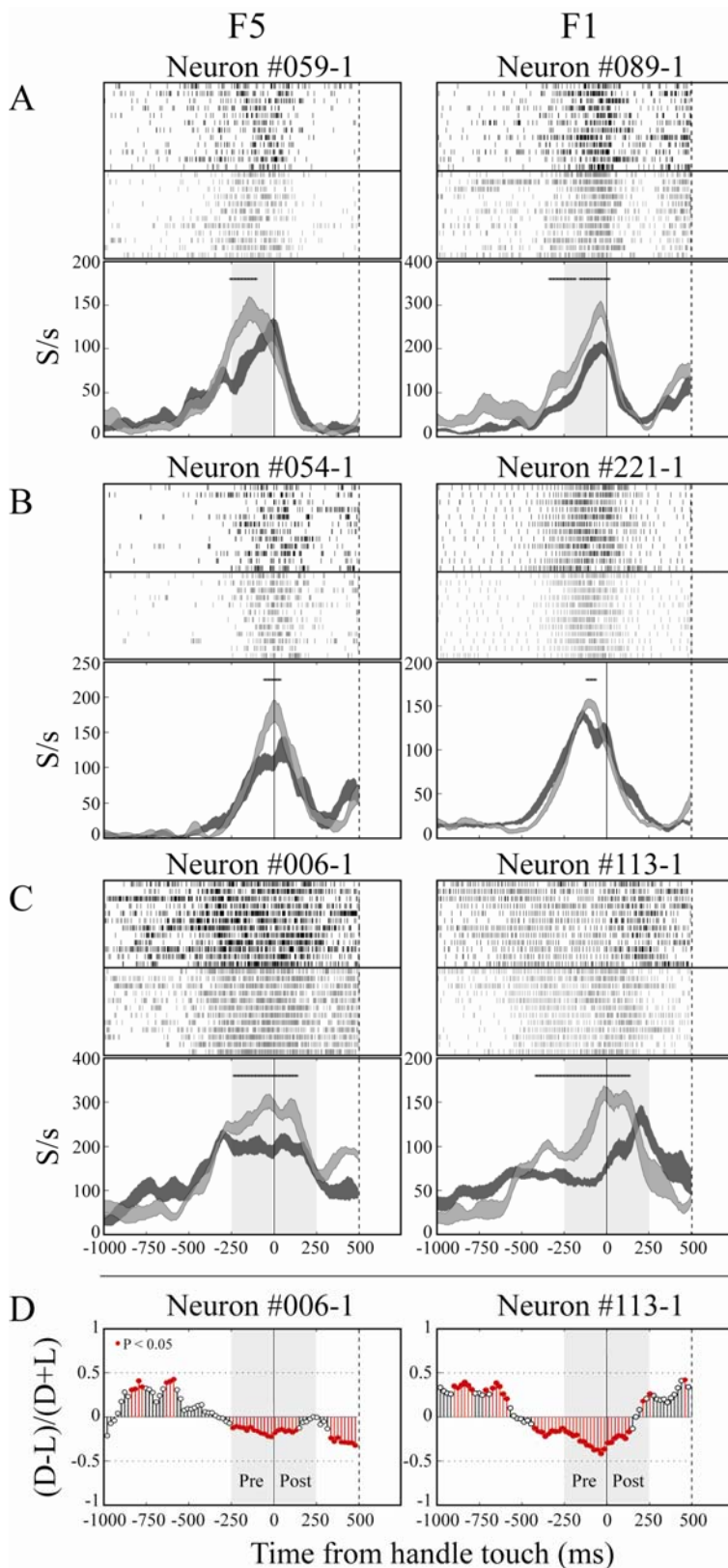


**Figure 5.** Single units exemplifying the most significant F5 and F1 neuronal categories determined by the running *t*-test analysis. The first 1500 ms of activity aligned to time of handle touch (solid line) are shown. Spike density plots are obtained by first smoothing each trial firing rate (spikes/sec, 5-ms bin width) by a Gaussian kernel function (20-ms window width) and then averaging across trials within each condition. Ribbons represent mean single-neuron response  $\pm$  1 S.E.M. in the *L* (grey) and *D* (black) condition. Symbols on top indicate trial bins where *t*-test result was significant

(5% alpha level). Top raster plots represent the respective spike trains recorded from the neuron in the 12 trials of the *L* and *D* conditions. A: Neurons showing  $L > D$  modulation in the *pre-touch* sub-epoch (shaded area). B: *L*-modulated neurons around the instant at which the hand touched the handle. C: Neurons expressing *L*-selectivity in both *pre-* and *post-touch* sub-epochs (shaded areas). D: Stem plots exemplifying the running *t-test* analysis performed on the *L-* and *D-*related activity of the neurons shown in (C). The activity of the neurons in the two conditions is represented by the index  $(D-L)/(D+L)$ ; lines extending from the baseline (index = 0) upward and downward respectively represent  $D > L$  and  $L > D$  modulations computed at each 100-ms bin. Red and black lines indicate significant and non-significant modulations, respectively. A given neuron was considered as *L-* or *D-*selective if it displayed the same significant modulation in at least two consecutive bins. The same analysis was performed also to detect *PT flash/T flash*-selective neurons.

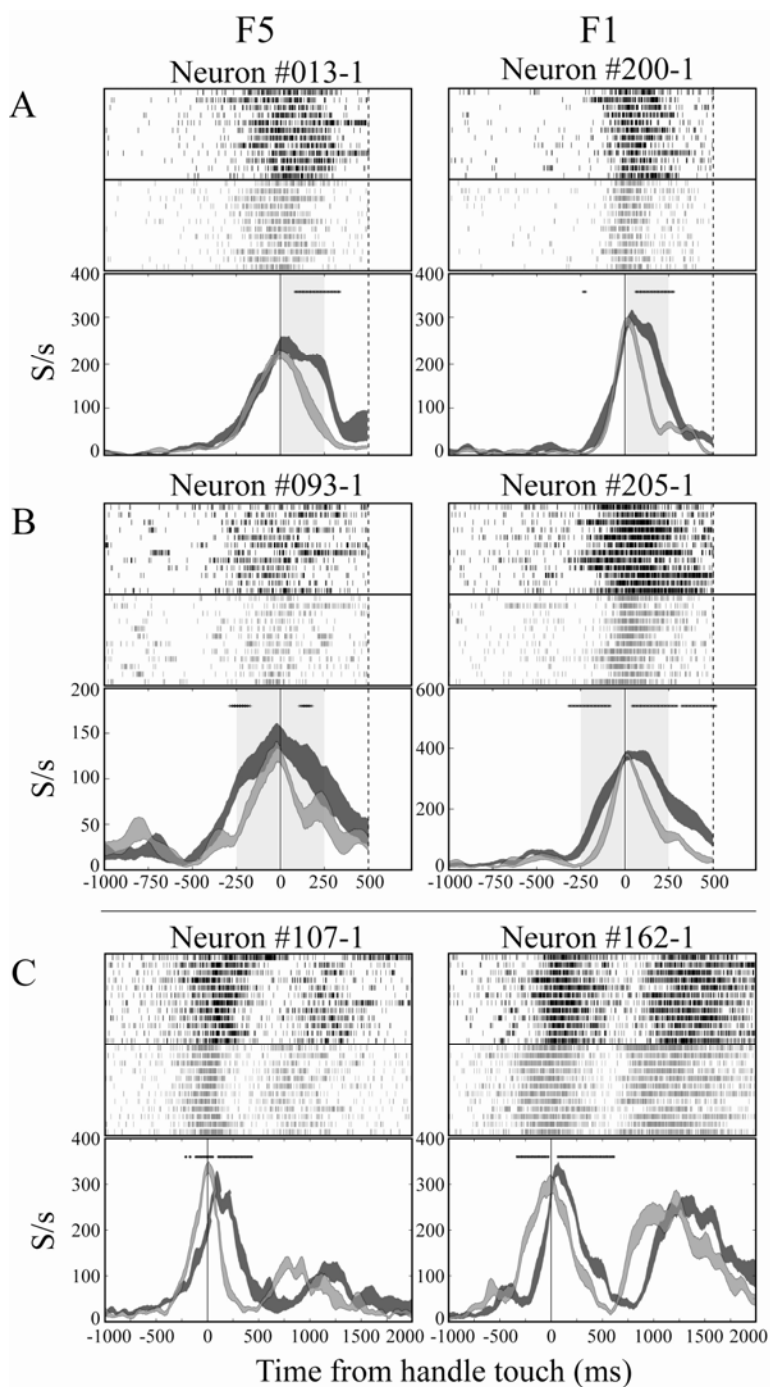


**Figure 6.** Single units exemplifying other significant F5 and F1 neuronal categories determined by the running *t-test* analysis. A: Neurons showing a  $D > L$  modulation in the *post-touch* sub-epoch (shaded area). B: Neurons with higher firing rates in the *D* condition throughout *epoch 2* (shaded areas). C: Neurons with *spurious* effect, exhibiting opposite modulations within *epoch 2*, as a result of a shift in activity between *L* and *D* conditions. Conventions as in Fig. 5.

the grasping activity of three different units of F5 and of F1 are illustrated in Figure 5. Full vision of the ongoing action made these neurons discharge more, compared to the full dark condition, either during the hand shaping phase of grasping (Fig. 5A), or at the contact time between the hand and

the door handle (Fig. 5B) or throughout all *epoch 2*, including the very final phase of grasping (Fig. 5C). It is worth noting that these light-induced modulations were mainly expressed as additive effects to the basic motor activity of the neurons recorded in the dark; indeed, the decaying part of the discharge profile of both F5 and F1 units in Figure 5A overlapped in the two conditions and so did the ascending and descending phases of the grasping activity of the other single-neuron examples in Figure 5.

In contrast, the modulated activity of neurons in Figure 6A was of a rather different kind; these units exemplify the firing behavior of a large fraction of neurons showing a significant  $D>L$  effect which was actually the result of a more prolonged *post-touch*  $D$ -related response, likely associated with hand tactile/proprioceptive adjustments after the monkey's hand reached the handle under full dark conditions. In contrast, the response recorded in the  $L$  condition rapidly decayed after touch. The same observation holds for neurons in Figure 6B, displaying an overall more spread-out grasping activity in the  $D$  than in the  $L$  condition (with no difference at the peak activity). Single neurons in Figure 6C were largely represented both in F5 (16%) and F1 (23%) and showed a clear rightward temporal shift in the grasping response recorded in the dark, compared to that observed in the light. This was particularly evident at the discharge peak and resembled that often recorded during the following grasping of the food (see last 1500 ms of plots in Fig. 6C), when no experimental control was imposed to ensure that the movement in the dark could be performed by the monkey as accurately as the movement in the light. Statistical analysis run on these neurons returned a  $L>D$  (or, to a lesser extent,  $D>L$ ) effect in the *pre-touch* sub-epoch followed by the reverse modulation in the *post-touch* sub-epoch (see "*Spurious*" entry in Table 1). Since we were mainly interested in identifying neurons showing a true  $L$ -related potentiation (amplitude increase) of motor activity and one can hypothesize that the timing difference just described might be strictly related to a difference in  $D/L$  hand kinematics, neurons of this kind were considered as a separate class, thus not influencing neither the number of cells showing a *pre-touch*  $L>D$  modulation, nor the group displaying higher activity in the dark during the *post-touch* sub-epoch.

#### *Pre-touch light-responsive neurons in areas F5 and F1*

Of all the cells which were light-responsive in the different temporal phases of grasping, the neuronal subset discharging more in  $L$  than  $D$  condition during the *pre-touch* sub-epoch was the largest one (see Fig. 4). This result is of remarkable interest for the purpose of the current work, since it suggests that, although visual information on the ongoing movement was continuously

available in the *L* condition, the activity of both F5 and F1 grasping neurons was particularly modulated just in the period when the shaping of the hand preceding grasping was taking place.

In the following paragraphs this particular class of cells will be analyzed in detail.

*F5 and F1 pre-touch light-modulations had similar time course and strength*

Figure 7A shows the time course of normalized *L* and *D* average activity of *pre-touch* light-responsive cells in areas F5 and F1. If one considers the temporal build-up of the light-effect, these two populations did not show any substantial difference. In both cases, the curves depicting *L*- and *D*-related grasping activity started separating in a statistically significant way (two-tail paired *Student's t-test*, 5% alpha level) at the 100-ms bin centered at 270 ms before handle touch. This similarity in the latency of light-selectivity was also confirmed by the time to half-maximum divergence in activity computed on the normalized mean firing rate differences in the sliding 100-ms window. This method returned a peak of *L* vs. *D* discharge difference in the bin centered at 80 ms prior to touch in both areas, with the half-value of this peak achieved by F5 and F1 neurons at 210 and 190 ms before touch, respectively (Fig. 7B).

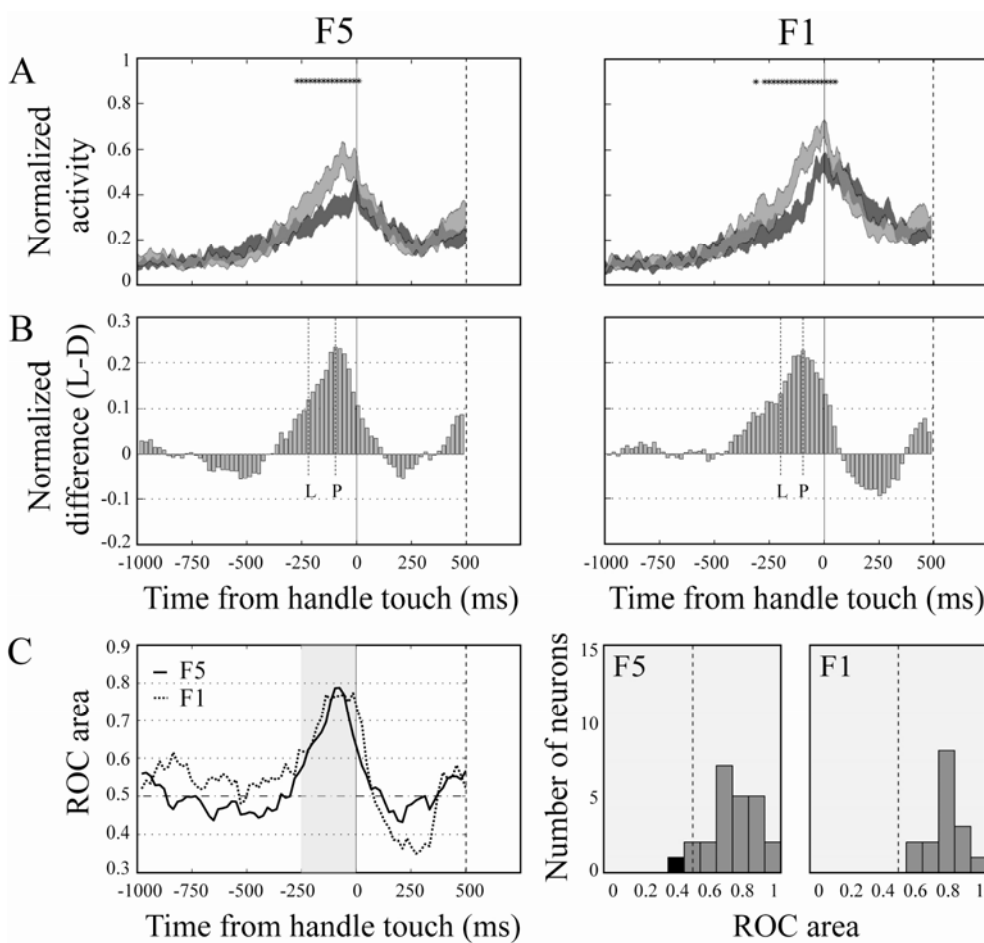


**Figure 7.** A: Average activity of *pre-touch* light-responsive neurons in area F5 and F1. The first 1500 ms of activity aligned to time of handle touch (solid line) are shown. Population spike density plots are obtained by first normalizing the single-neuron smoothed data (Gaussian kernel function with window width set to 30 ms) to the absolute maximum level of activity observed across all 4 different conditions and then averaging the result across all units in the populations. Traces represent the population *L*- (grey) and *D*- (black) related average response  $\pm 1$  S.E.M.. Symbols on top indicate trial bins where the running *t*-test result was significant (5% alpha level). B: Time course of the respective F5 and F1 population normalized *L*-*D* discharge differences, computed on a sliding 100-ms bin, shifted by 20-ms steps. Temporal peak and latency of light-selectivity (calculated as the times to maximum and to half-maximum difference in activity) are respectively represented by the P- and L-labeled dashed lines within each plot. F5 and F1 populations reached the latency (bin centered at 210 and 190 ms before touch, respectively) and peak (bin centered at 80 ms before touch, in both plots) of selectivity almost at the same time. C (left): Time course of ROC values for the *pre-touch* light-selective neurons in area F5 and in area F1. The first 1500 ms of activity aligned to time of handle touch (solid line) are shown. Traces are obtained averaging across neurons the area under the ROC curve, computed every 20-ms step and comparing *L* and *D* firing rates in a sliding 100-ms bin. C (right): Histograms showing the distribution of F5 and F1 single-neuron ROC area values in the *pre-touch* sub-epoch (corresponding shaded area in the upper plot A). ROC areas greater than 0.5 (grey) indicate neurons conveying more light- than dark-related information; ROC values less than 0.5 (black) represent neurons expressing higher activation in the *D* than in the *L* condition. Note that the presence of black bars is due to the criterion used for selecting light-responsive neurons, requiring selectivity in at least 2 consecutive 100-ms bins of *pre-touch* sub-epoch.

In addition, the strength of light-responsiveness displayed by the two neuronal subgroups, aside from some minor differences, was almost comparable. The magnitude of the *L*-effect over time was measured by computing the population mean ROC area for the two conditions on each 100-ms bin stepped on the trial. Figure 7C (left) shows that F5 and F1 light-responsiveness developed in a similar way around the handle grasping period, though F1 selectivity was overall stronger. However, F5 light-modulation was slightly higher at the peak. The distribution of *pre-touch* ROC area values across neurons in the F5 and F1 subgroups (Fig. 7C, right) confirmed that, even though statistically similar (*Student's t*-test, n.s.), the light-sensitivity level during the hand shaping phase of grasping was on average higher in F1 ( $0.799 \pm 0.023$ ) than in F5 ( $0.746 \pm 0.032$ ).

*Unlike F1 neurons, F5 neurons showed significantly different response profiles under light and dark conditions*

Although numerically equivalent and showing a *L*-modulation with comparable time course and magnitude, F5 and F1 populations differed substantially one from the other in regard to the discharge profile displayed during the *L* and *D* conditions. In particular, despite the fact that the *L*- and *D*-related activity profiles started diverging at the same time in the two areas, in the F1 recorded

population  $L$  and  $D$  profiles grew up and reached the peak almost in parallel, while in area F5 they developed with clearly different slopes.

Figure 8A shows the average temporal peak and latency of the F5 and F1 motor response (detailed values are reported in Table 3). It is important to point out that latency, since computed as the time to half the discharge peak, is more associated to the rise time to the peak of activity, rather than just to the onset of the grasping response. In contrast to the F1 population, showing no timing difference in the grasping activity between the two conditions (two-tail paired *Student's t-tests*, not significant at 5% alpha level), the mean peak and latency times of the F5 neuronal response in the  $L$  condition were significantly shorter than those observed in the  $D$  condition. Overall, F5 *pre-touch*  $L$ -sensitive neurons peaked much earlier in full light ( $-94 \pm 25$  ms, mean  $\pm$  S.E.M.), than in full dark ( $-47 \pm 29$  ms) ( $t = 2.3$ ,  $P = 0.03$ ). They also displayed a much faster ramping activity to the peak in full light ( $-135 \pm 27$  ms) than in full dark ( $-81 \pm 30$  ms) ( $t = 2.7$ ,  $P = 0.01$ ), as revealed by the time-to-half-the-maximum parameter.

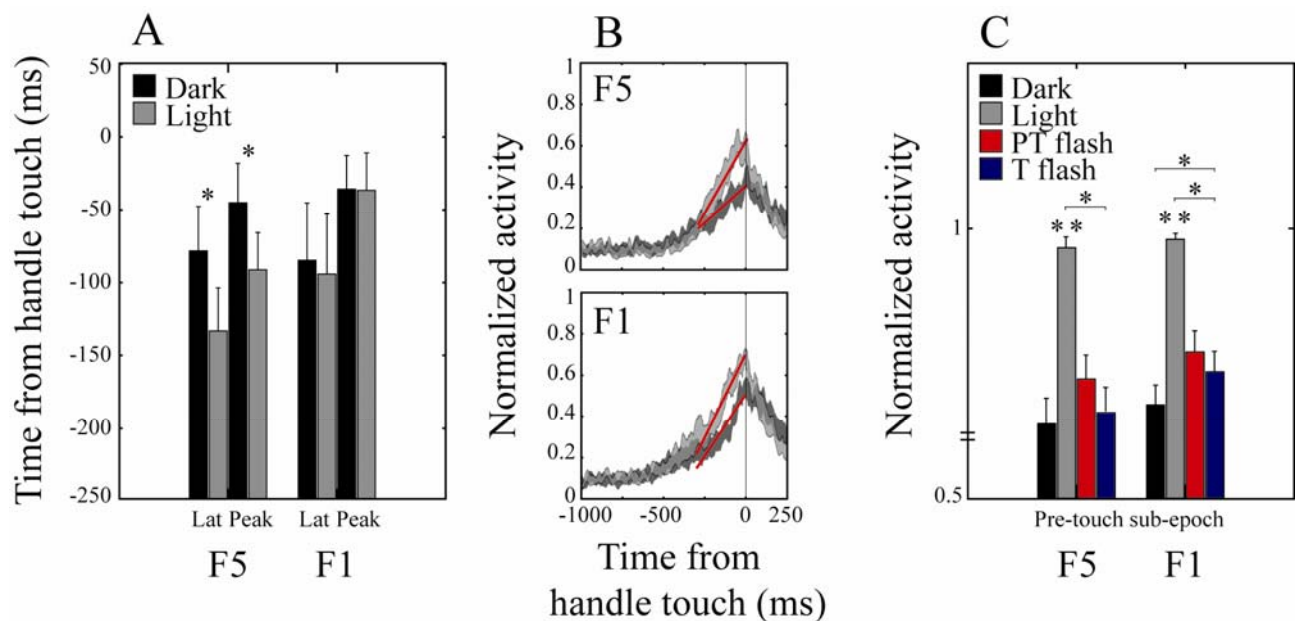


**Figure 8.** A: Mean latency and peak times for the  $L$ - (grey) and  $D$ - (black) related responses of F5 and F1 *pre-touch*  $L$ -selective populations. Note that latency is computed as the time to half the peak of discharge, meaning that it is more related to the rise time of activity to the peak, rather than to the actual onset of the neuronal response. Asterisks on top indicate statistically significant differences (*Student's t-test*, 5% alpha level). B: Line fitting of the  $L$ - and  $D$ -related response of F5 and F1 *pre-touch*  $L$ -selective neurons in the 300-ms window prior to touch. The regression analysis returned similar slope-intercept  $L$  and  $D$  functions for the F1 population, while F5 population displayed very different ramping activities: the median slope of the  $L$  and  $D$  response profiles was respectively  $57.1^\circ$  and  $40^\circ$  for F5 neurons and  $63.7^\circ$  and  $49.4^\circ$  for F1 neurons. C: Average activity of F5 and F1 *pre-touch*  $L$ -responsive neurons during *pre-touch* sub-epoch in the four experimental conditions. Asterisks on top of bar plots indicate main significant differences among conditions ( $P < 0.05$ , LSD post-hoc tests, subsequent to significant one-way ANOVA *condition* main effect).

**Table 3.** Average timing parameters of the *D*- and *L*-related response profiles of F5 and F1 *pre-touch* *L*-selective populations.

	<i>Latency (ms)</i>	<i>Peak (ms)</i>
<b>F5</b>		
Light	-135 ± 27	-94 ± 25
Dark	-81 ± 30	-47 ± 29
<b>F1</b>		
Light	-96 ± 23	-39 ± 26
Dark	-87 ± 39	-38 ± 41

Values are mean times from handle touch (ms) ± 1 S.E.M.

The half-peak timing difference could not be explained by the amount of *L*-selectivity of the F5 neurons: in addition to the fact that F5 neurons were as *L*-selective as F1 neurons (see above), the discharging difference between the two conditions in the *pre-touch* sub-epoch did not significantly correlate with the difference in latency ( $r = 0.2$ ;  $P = 0.2$ ). The difference found in the peaking times between the two conditions well supports this observation, since it could not be at all related to the significant *pre-touch* divergence between the *L* and *D* discharge profiles.

To better describe this temporal profile difference, a linear regression function interpolating the activity of each cell of the F5 and F1 *pre-touch* *L*-selective populations in a 300-ms window prior to touch (i.e., going from -300 to 0 ms and representing the most significant portion of the *pre-touch* neuronal response) was computed for each of the *L* and *D* condition. Neurons showing a negative slope regression parameter  $m$  (i.e., the first derivative) in both conditions, thus characterized by a substantially different response profile, were discarded from average. Whereas in the F1 population ( $n = 13$ ) the slope regression parameter of the *L* (median  $m = 63.7^\circ$ , Inter-Quartile Range, IQR =  $11.4^\circ$ ) and *D* ( $m = 49.4^\circ$ , IQR =  $16.4^\circ$ ) ramping activities was approximately comparable (*Wilcoxon signed ranks test*,  $W^+ = 1.6$ , n.s.), in the F5 population ( $n = 20$ ) it substantially changed (*L*,  $m = 57.1^\circ$ , IQR =  $33.8^\circ$ ; *D*,  $m = 40^\circ$ , IQR =  $31.7^\circ$ ;  $W^+ = 2.8$ ,  $P = 0.003$ ). Figure 8B shows population fitting line plots for the average *D* and *L* response profiles of F5 and F1 *pre-touch* *L*-selective neurons.

Importantly, none of the F5 and F1 neurons which were *L*-responsive in either of the other considered sub-epochs displayed such a significant timing difference between the *L* and *D* response profiles, indicating that this result was highly specific for the *pre-touch* *L*-selective neuronal population recorded from area F5. In addition, the motor discharge of the F1 *pre-touch* neurons in the *L* condition was consistently, though not significantly (*Student's t-test*, 5% alpha level), delayed (39 and 55 ms at the latency and peak, respectively; see Table 3) with respect to that of the F5 population, suggesting a functional interplay between the two areas.

Taken together, these results strongly indicate that the *L*-modulation of the *pre-touch L*-responsive F5 neurons, in contrast to that of F1 neurons, mainly consisted in a temporal gain of the *L*-related response over the *D*-related response. This was achieved through a faster increase of the *pre-touch* activity when the monkeys could observe their own hand during the shaping phase of grasping compared to when they could not.

*F5 and F1 pre-touch light-responsive neurons were overall not modulated by flash conditions*

Multiple LSD post-hoc comparisons performed on the significant main effect ( $P < 0.05$ ) of a one-way (*condition*) ANOVA computed on the *pre-touch* sub-epoch activity of each neuron were used to test whether F5 and F1 *pre-touch L*-responsive neurons were also modulated by the transient visual feedback of the *flash* conditions. Only 2 out of the 24 F5 *pre-touch L*-selective neurons (1% of the total number of F5 neurons) displayed a significantly different response in the two *flash* conditions and the activity recorded in the *flash* condition for which they expressed selectivity was higher than that observed in full dark. None of the F1 *pre-touch L*-selective neurons showed such a combined effect. Instead, the firing rate displayed by the majority of F5 (79%) and F1 (63%) *pre-touch L*-responsive neurons in the *flash* conditions was as high as that recorded in the *D* condition, and for all neurons the activity exhibited during the *L* condition was significantly higher than that measured during *flash* and *D* conditions. Figure 8C shows the average discharge of the F5 and F1 *pre-touch L*-responsive populations in the *pre-touch* sub-epoch during the four different conditions: for both populations, the activity in the *L* condition was significantly higher than that observed in *D*, *PT flash* and *T flash* conditions ( $P < 0.01$ ) and no difference was detected between flashes.

These last results suggest that in both areas, the transient visual information available at flash presentation was not as effective as the continuous vision of the own ongoing grasping movement in enhancing the activity of the *pre-touch L*-responsive neurons.

*PT flash vs. T flash conditions: selectivity for specific transient visual feedbacks*

To identify neurons showing selectivity for either of the two transient visual feedback conditions, the activity recorded during the *PT flash* condition was directly contrasted with that observed during the *T flash* condition. The running *t-test* analysis (see *Methods*) revealed a large portion of both F5 (48%) and F1 (43%) neurons selectively modulated by the transitory vision of the own ongoing action during specific grasping phases, namely hand shaping (F5: 19%; F1: 22%) or hand-object contact (F5: 29%; F1: 21%) (Table 4). Neurons significantly increasing their activity in response to both *PT flash* and *T flash* presentation within *epoch 2* were very few (4% in area F5 and 1% in area F1) and were not taken into consideration for the analyses. Figure 9 shows examples

of single flash-responsive neurons drawn from the F5 and F1 populations. These neurons specifically increased their activity during the grasping period of *PT flash* (Fig. 9A) or *T flash* (Fig. 9B) condition, respectively.

**Table 4.** Summary of results from the running paired *t-test* analysis comparing single-neuron activity in *PT flash* vs. *T flash* condition in a 100-ms bin shifted through the trial by 20 ms steps.

	<i>Epoch 2</i> (-250 ms – 250 ms)		<i>Pre-touch</i>	<i>Touch</i>	<i>Post-touch</i>	<i>Pre- + Post-touch</i>	<i>Sub-total</i>
	MK1	MK2					
Intersection with <i>L</i> -selective neurons							
<b>F5</b>							
PT flash-selective	23	9					
	32 (19%)		4	--	--	--	4 (2%)
T flash-selective	29	20					
	49 (29%)		5	--	4	1	10 (6%)
<i>Modulated</i>	81 (48%)						
<i>Non-selective</i>	50	38					
	88 (52%)						
<b>Total</b>	<b>169 (100%)</b>						
<b>F1</b>							
PT flash-selective	24	5					
	29 (22%)		1	--	1	1	3 (2%)
T flash-selective	23	4					
	27 (21%)		6	--	1	--	7 (5%)
<i>Modulated</i>	56 (43%)						
<i>Non-selective</i>	72 (57%)						
<b>Total</b>	<b>128 (100%)</b>						

Neurons are divided according to the monkey from which they were recorded (MK1 or MK2) and the specific flash-selectivity they showed in *epoch 2*. Intersection of each flash-selective neuronal group with *L*-selective neurons in the different time epochs (see table 1) is also shown. The percentage values always refer to the entire sample of recorded neurons.

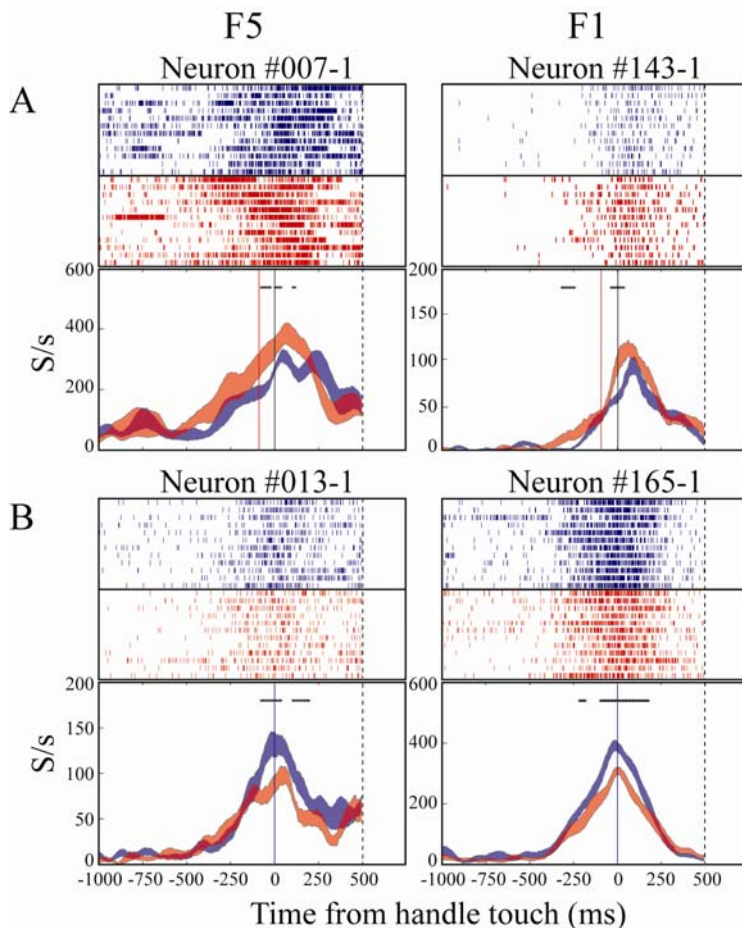


**Figure 9.** Examples of F5 and F1 flash-responsive single neurons, as returned by the running *t-test* analysis. A: Neurons showing significantly higher firing rates during *epoch 2* of the *PT flash* condition (red) than during *epoch 2* of the *T flash* condition (blue). B: neurons specifically responding to *T flash*. Red and blue dashed lines represent the time of *PT flash* (-91 ms in the F5 neuron and -96 ms in the F1 neuron) and *T flash* (always at 0 ms) occurrence. Other conventions as in Fig. 5.

*F5 and F1 flash-modulations were displayed according to the grasping phase at which the transient visual information was delivered*

Figure 10 shows the time course of *PT flash* and *T flash* average activity of the specific flash-responsive F5 and F1 populations. For both areas, the temporal build-up of the flash effect varied consistently between the *PT* and *T flash*-responsive groups, in accordance with the different grasping time at which the flash was delivered. Specifically, the two flash-related activity curves began diverging much earlier in the *PT* than in the *T flash*-selective neuronal groups: F5 and F1 *PT flash*-responsive neurons started firing significantly higher (two-tail paired *Student's t-tests*, 5% alpha level) in the *PT flash* condition at the 100-ms bin centered respectively at -430 and -410 ms

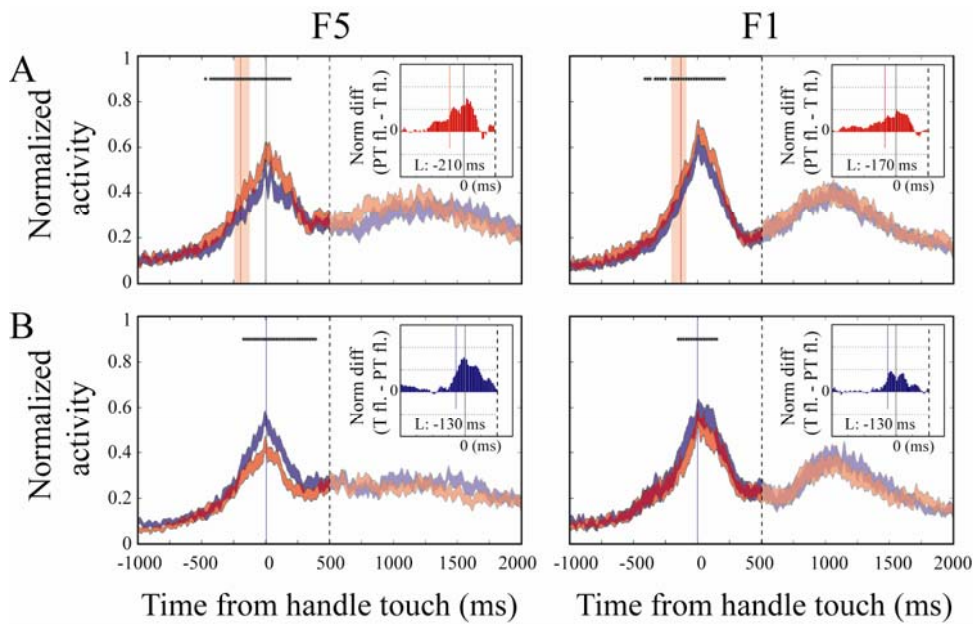


**Figure 10.** Average activity of flash-responsive neurons in area F5 and F1. Activity in *PT flash* (red) is plotted vs. activity in *T flash* (blue) condition. A: *PT flash*-selective populations. Red dashed lines and red shaded areas respectively represent the median time of *PT flash* occurrence and respective interquartile range (-201 ms, IQR = 115 ms in the F5 population; -133 ms, IQR = 113 ms in the F1 population). B: *T flash*-selective populations. Blue dashed lines represent the time of *T flash* occurrence (always at 0 ms). Other conventions as in Fig. 7A.

Inset plots show time course of population normalized *flash*-related discharge differences, computed on a sliding 100-ms bin, shifted through the first 1500 ms in the trial by 20-ms steps. Latency of flash-selectivity (calculated as the time to half-maximum difference in activity) is represented by the L-labeled dashed line within each plot. Flash-selectivity latency of both F5 and F1 *PT flash*-responsive populations (bin centered at 210 and 170 ms before touch, respectively) was shorter than that of F5 and F1 *T flash*-responsive populations (bin centered at 130 ms before touch, in both plots). X- and y-axis scales as in Fig. 7B.

before handle touch, even well in advance of flash delivery, respectively occurring at around -201 ms and -133 ms. This latter difference in flash presentation was related to the fact that F5 neurons were recorded from both hemispheres of the same monkey, forced to reach and grasp first with the right and then with the left hand, and that left-hand movements were much slower than the right-hand ones (details concerning the time of *PT flash* presentation are reported in Table 1). In contrast, the first time window in which both the F5 and F1 *T flash*-responsive groups showed significantly enhanced *T flash* activity was respectively centered at -170 and -150 ms. In this case, flash selectivity was observed much later than in the *PT flash*-selective populations, though again clearly before the hand-handle contact, triggering *T flash* presentation (occurring at 0 ms). This anticipatory flash-related response of the neurons was likely dependent on the experimental design, implying a blocked presentation of conditions, so that the time of flash presentation within one specific flash trial block could be expected, and thus predicted. The difference in latency of the two specific flash-

related modulations was confirmed by computing the time to half-maximum divergence in activity between the two flash conditions, which was shorter for the *PT flash*-responsive neurons (F5: -210 ms; F1: -170 ms, see inset plots in Figure 10A) than for those specifically sensitive to *T flash* (F5: -130 ms; F1: -130 ms, see inset plots in Figure 10B).

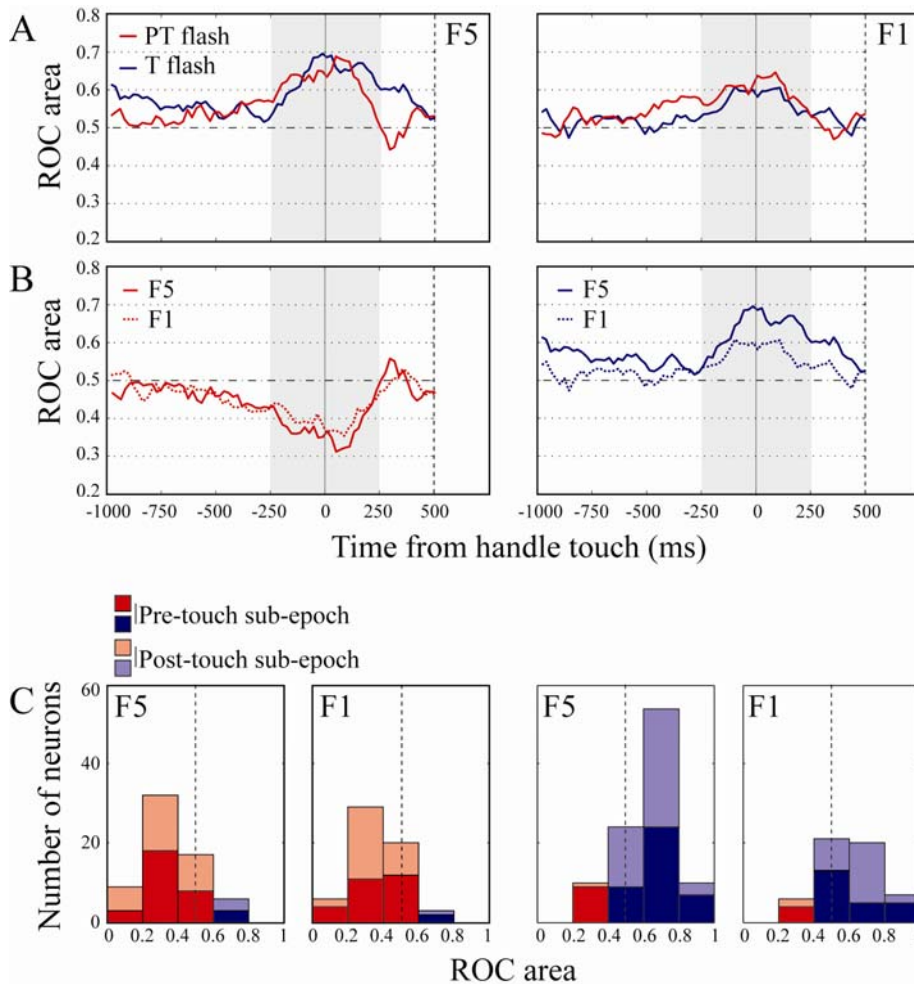


**Figure 11.** A: Time course of ROC values for *PT* (red) and *T* (blue) *flash*-selective neuronal groups in area F5 and F1. The first 1500 ms of activity aligned to time of handle touch (solid line) are shown. Traces are obtained averaging across neurons the area under the ROC curve, computed every 20-ms step and comparing *PT flash* and *T flash* firing rates in a 100-ms bin covering all the trial. Both traces are represented with positive ROC values to better contrast them. B: Same traces as in (A) but grouped according to type of flash selectivity (left plot: *PT flash*-responsive neurons; right plot: *T flash*-responsive neurons), to emphasize differences between areas. C: Histograms showing the distribution of single-neuron ROC area values in both *pre-touch* (dark blue and dark red) and *post-touch* (pale blue and pale red) sub-epochs within *PT flash*- and *T flash*-responsive groups recorded from the two brain regions. ROC areas greater than 0.5 (blue) indicate neurons conveying more *T flash*- than *PT flash*-related information; ROC values less than 0.5 (red) represent neurons expressing the opposite effect. Note that the presence of bars of the opposite color within each plot is due to the criterion used for selecting flash-responsive neurons, not requiring selectivity through all *epoch 2* but at least in 2 consecutive 100-ms bins of it.

Close examination of the time course of the modulations, as processed by the ROC analysis (Fig. 11A), revealed a clear-cut temporal shift of the flash effects in area F5, specifically depending on the time of flash presentation (Fig. 11A: compare ROC for F5 *PT flash*-selective neurons, in red, and ROC for F5 *T flash*-selective neurons, in blue). The time course of *PT flash*-related selectivity was characterized by a gradual increase during the pre-shaping phase of grasping, followed by a fast decay immediately after touch. Conversely, *T flash*-related selectivity increased rapidly before touch, reached the highest value at the hand-handle contact and declined slowly in the *post-touch* sub-epoch, persisting throughout the final phase of grasping. According to the running *t-test* analysis, the *PT flash* effect became manifest 260 ms earlier than the *T flash* effect; likewise, it also disappeared 200 ms earlier (the *PT* and *T flash* last significant bins were respectively centered at 190 ms and 390 ms after touch, see Fig. 10A).

The latencies of *PT* and *T flash* signals in area F1 showed a time lag (200 ms) comparable to that observed in the activity of F5 flash-responsive neurons. However, in contrast to F5, F1 *T flash* effect was more temporally locked to the handle touch instant, decaying 60 ms earlier than the *PT flash* effect (see Fig. 10B and Fig. 11A).

#### *Flash-related signals were stronger in area F5 than in area F1*

Flash-related information conveyed by F5 neurons within *epoch 2* was overall higher than that of F1 neurons, especially considering *T flash* selectivity. This was visible when comparing the time course of ROC values of the flash-responsive groups recorded from the two brain regions (Fig. 11B).

*PT flash*-selectivity in F5 was overlapping in strength that of F1 during the pre-movement period (*epoch 1*); then, around 250 ms before handle touch, it reached a higher level which was maintained for all the *pre-touch* sub-epoch and till about 100 ms after touch. Even more evidently, *T flash*-selectivity in F5 started increasing approximately at the same time (-250 ms) as the one observed in F1, nevertheless diverging considerably from it around 100 ms prior to hand-object contact. This ROC area difference then remained through all *touch* and *post-touch* sub-epochs, only decaying after the grasping movement was concluded (at around 450 ms after touch). Accordingly, although overall not statistically different (*Student's t-test*, 5% alpha level), the ROC area values expressed by F5 *T flash*-selective single neurons were higher than those measured in the *T flash*-responsive population of F1, both during the *pre-touch* (F5,  $0.623 \pm 0.028$ ; F1,  $0.594 \pm 0.034$ ) and the *post-touch* (F5,  $0.644 \pm 0.019$ ; F1,  $0.616 \pm 0.03$ ) sub-epochs (Fig. 11C). Seemingly, average ROC area measured in *PT flash* neurons was higher in area F5 (*pre-touch* sub-epoch:  $0.364 \pm 0.025$ ;

*post-touch* sub-epoch:  $0.354 \pm 0.032$ ) than in area F1 (*pre-touch* sub-epoch:  $0.376 \pm 0.029$ ; *post-touch* sub-epoch:  $0.36 \pm 0.027$ ).

### F5 and F1 flash-selective neurons were overall not light-responsive

The majority of both F5 and F1 flash-selective neurons did not show any significant light responsiveness. Only a small fraction of *PT flash*-responsive neurons (2% in both F5 and F1 area) and *T flash*-responsive neurons (5% in F5 and 6% in F1) displayed significantly higher firing rates in full light than in full dark and mainly during the *pre-touch* sub-epoch (see Table 4). Therefore, flash-selective neurons formed relatively mixed populations with regard to the behavior they expressed in *L* and *D* conditions, with a relevant portion of them pertaining to non-selective or *D>L* populations (overall, 21% and 11% in F5 and F1, respectively). Figure 12 shows the average activity of each flash-selective population in all four experimental conditions along the trial.

To better weight the flash selectivity of these populations against the activity shown in *D* and *L* conditions, a one-way ANOVA with *condition* (*D*, *L*, *PT flash* and *T flash*) as factor was performed on the response of each flash-responsive neuron acquired during the epoch (*epoch 2*), in relation to which flash-selectivity was determined. A large amount of both F5 (37/81: 46%) and F1 (31/56: 55%) *flash*-selective neurons showed significantly higher firing rates in the *flash* condition for which they were selective than in both *D* and *L* condition, as well as than in the other flash condition.

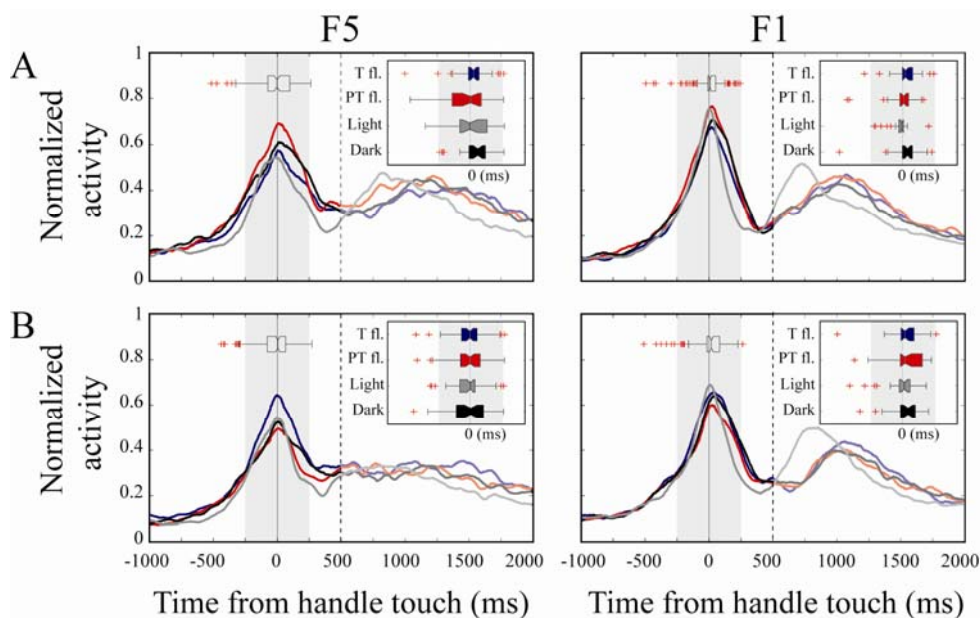


**Figure 12.** Average activity of flash-responsive neurons in area F5 and in area F1. Activity is aligned to time of handle touch (solid line). Population spike density plots are obtained by first normalizing the single-neuron smoothed data (Gaussian kernel function with window width set to 100 ms, to better emphasize the neuronal response profile) to the absolute maximum level of activity observed across all 4 different conditions and then averaging the result across all

units in the populations. Average activity in *PT flash* (red), *T flash* (blue), *L* (grey) and *D* (black) conditions is plotted for each group. A: *PT flash*-selective populations. Box plots on top indicate the temporal distribution of the discharge peaks of the neurons within a population. The distance between left and right limits of the box define inter-quartile range (IQR) of the sample, which is a robust estimate of the dispersion of the data. The line in the middle is the sample median, whiskers represent the extent of the rest of the data and red crosses are outliers. Inset plots show the temporal spread of the discharge peaks of each flash-selective group in the four conditions. IQR details are given in table 5. Grey-shaded areas represent *epoch 2* on which the one-way ANOVA (see main results in Fig. 13A) has been performed.

The same analysis was performed also at the population level. Figure 13A illustrates the main statistical results: *PT flash*-responsive neurons of both areas F5 and F1 (left bar groups in the respective plots) showed the strongest grasping response during the *PT flash* condition (firing rates recorded during the other experimental conditions were significantly lower;  $P < 0.05$ , ANOVA LSD post-hoc tests). In addition, F5 *PT flash*-selective neurons fired significantly more in full dark than in full light ( $t = 3.4$ ,  $P = 0.002$ ) or when a light flash was delivered at the handle touch ( $t = 2.6$ ,  $P = 0.01$ ). F1 *PT flash*-selective neurons showed a significant  $D > L$  effect ( $t = 2.1$ ,  $P = 0.04$ ) as well. Similarly, *T flash*-related discharge of the F5 *T flash*-responsive population (Fig. 13A, F5 right bar group) was much higher compared to the activity displayed by the same neurons in *L*, *D* and *PT flash* conditions ( $P < 0.0001$ ). Conversely, F1 *T flash*-selective neurons (Fig. 13A, F1 right bar group) only showed a significant difference between the two flash conditions ( $t = 5.5$ ,  $P < 0.0001$ ).

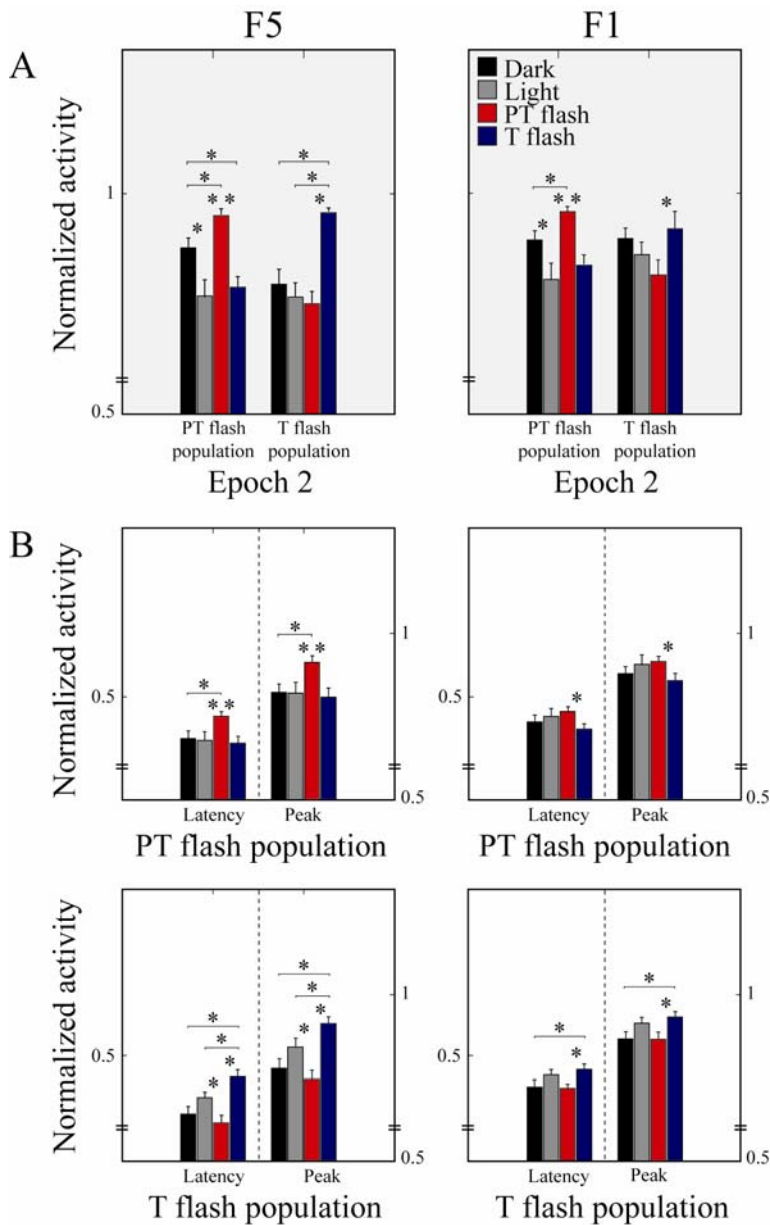


**Figure 13.** Average activity of *PT* and *T flash*-responsive neurons in area F5 and F1, both during *epoch 2* (A) and at the time of maximum (*Peak*) and half-maximum (*Latency*) discharge (B) in the four experimental conditions. Asterisks on top of bar plots indicate main significant differences among conditions ( $P < 0.05$ , LSD post-hoc tests, subsequent to significant one-way ANOVA *condition* main effect).

#### *Flash-related signals were more specific in area F5 than in area F1*

When looking at the population plots of the flash-selective neurons in the two recorded areas (Fig. 12), the following interrelated considerations can be drawn: first, the ANOVA results just described do not exactly reflect the level of neuronal activation expressed by the different populations in the grasping period of the four conditions, as it appears in the plots (see activity within shaded areas in Fig. 12). More precisely, the mean neuronal discharge in *epoch 2* (Fig. 13A)

does not seem to be the appropriate measure to explain the differences among conditions in the neurons' grasping-related response profiles, particularly in the case of area F1.

Second, the average response profile of the neurons assigned to the different flash-responsive groups varied a lot across areas and conditions. In particular, if considering the temporal distribution of the neurons' discharge peaks as an index of the population response profile variability (see Table 5 and inset box plots in Fig. 12), flash-selective cells of area F5 exhibited, on average, a rather spread-out grasping-related response (IQR = 144 ms), as opposed to the more compact one of the F1 flash-selective neurons (IQR = 71.5 ms). A dispersion test (*Ansari-Bradley test*, 5% alpha level) applied to F5 and F1 peak distributions revealed that the peaks dispersion was significantly different in the two areas ( $W^* = 5.8$ ,  $P < 0.0001$ ), particularly when contrasting the F5 and F1 *PT flash*-selective populations (IQR = 161 ms and 56 ms, respectively;  $W^* = 7.3$ ,  $P < 0.0001$ ). In contrast, the temporal dispersion in the activity peaks of the non-flash-responsive neurons was comparable in the two areas (F5 IQR = 125 ms; F1 IQR = 122.5 ms;  $W^* = 1.1$ , n.s.). Most importantly, the average response profile displayed by F5 flash-selective neurons across conditions specifically varied according to the flash condition for which they expressed selectivity (see inset box plots relative to area F5 in Fig. 12A and 12B). In particular, the firing dispersion shown by the F5 *PT flash*-responsive neurons in the *PT flash* condition (IQR = 214 ms) was significantly greater than that calculated in the same neurons during the *D* (IQR = 120 ms;  $W^* = 2.1$ ,  $P = 0.04$ ) and *T flash* (IQR = 78 ms;  $W^* = 2.9$ ,  $P = 0.003$ ) conditions. Conversely, the discharge peaks of the F5 *T flash*-selective neurons were consistently less dispersed in the *T flash* condition (IQR = 114 ms) than in the *D* (IQR = 199 ms;  $W^* = 1.9$ ,  $P = 0.05$ ) and *PT flash* conditions (IQR = 144 ms;  $W^* = 1.1$ , n.s.). Importantly, in both *PT* and *T flash*-responsive populations, the discharge peaks distribution observed during the flash condition for which the neurons were selective approached that assumed in the *L* condition (IQR = 199 ms and IQR = 112

**Table 5.** Temporal distribution of the discharge peaks of *PT* and *T flash*-selective populations in area F5 and F1. Median and inter-quartile range (IQR) are reported for each condition.

		<i>Peak IQR</i>	
		<i>(ms)</i>	
		<b>F5</b>	<b>F1</b>
Flash-selective neurons		144*	72
<b>PT flash-selective</b>		161	56
	<i>Dark</i>	120**	73****
	<i>Light</i>	199	34
	<i>PT flash</i>	214	65****
	<i>T flash</i>	78**	75****
<b>T flash-selective</b>		134	93

<i>Dark</i>	199	108
<i>Light</i>	112***	79
<i>PT flash</i>	144	160****
<i>T flash</i>	114***	96
Non-selective neurons	125	123

\* Significant difference (*Ansari-Bradley test* for samples with different dispersions, 5% alpha level) between F5 and F1 flash-selective neurons.

\*\* Significant differences with respect to *PT flash* condition within the same neuronal population.

\*\*\* Significant differences with respect to *Dark* condition within the same neuronal population.

\*\*\*\* Significant differences with respect to *Light* condition within the same neuronal population.

ms, respectively), which, in turn, differed substantially from that measured in the *D* condition (for details, see Tab. 5).

Opposite to what observed in area F5, the average response distribution of F1 flash-selective neurons in the flash condition on which they conveyed information was not significantly different from that of the *D* condition. Independently of the specific F1 flash-responsive population they were assigned to, these neurons showed firing peaks with similar temporal dispersion in the *PT flash*, *T flash* and *D* conditions. In all three conditions, a more spread-out neuronal response profile was observed, compared to that measured under full light conditions (see inset box plots relative to area F1 in Fig. 12A and 12B and Table 5).

Given these remarks, in order to have a more detailed picture of the grasping-related behavior of each specific neuronal population during the different experimental conditions, the following additional analyses were carried out: first, a one-way repeated-measure ANOVA was used to reveal differences in the absolute peak discharge values reached by the neurons within each condition. Main results are summarized in Figure 13B. For completion, firing rate differences among conditions assessed at the time to half-maximum activity (referred to as the latency) of the neurons are also reported for each population. As far as the *F5* flash-selective populations are concerned, this analysis confirmed the ANOVA results obtained considering all *epoch 2* (Fig. 13A). In addition, it revealed a significant  $L > PT \text{ flash}$  effect in the mean latency ( $t = 2.4$ ,  $P = 0.02$ ) and peak ( $t = 2.4$ ,  $P = 0.02$ ) activity of the *T flash*-selective neurons, emphasizing the strong *T flash* information carried by this population, also due to the suppression of the *PT flash*-related signal. On the contrary, the F1 flash-responsive groups did not show any distinct peak predominance of the specific flash condition for which they showed selectivity over all the other conditions, especially in the case of *PT flash*-selective neurons. *Touch flash* maximum activity of F1 *T flash*-responsive neurons was higher than that of *PT flash* and *D* conditions ( $P < 0.01$ ), but not significantly different from that measured in the *L* condition ( $t = 1.4$ ,  $P = 0.2$ ).

Second, to evaluate the average peak response in each condition also taking into account the corresponding population temporal peak distribution, the peak discharge of each neuron was weighed to the peak times of all the other neurons belonging to the same population (see *Methods*). A further one-way ANOVA was then used to test the differences among the new peak-related weighed values calculated for each condition. Main results are illustrated by bar plots in Figure 14. This analysis returned an important result regarding the *PT flash*-responsive neurons in F5. Contrary to what was obtained in the previous statistical analyses, the average weighted maximum response computed in the *PT flash* condition was not significantly higher than that measured in the *D* condition (see Fig. 14, *Latency* and *Peak* of the F5 *PT flash* population). However, as reported above, this neuronal group was the only one to show an increase, rather than a decrease, in the temporal dispersion of the firing peaks during the flash condition for which selectivity was conveyed. This evidence, besides suggesting that the appearance of a light flash during the hand

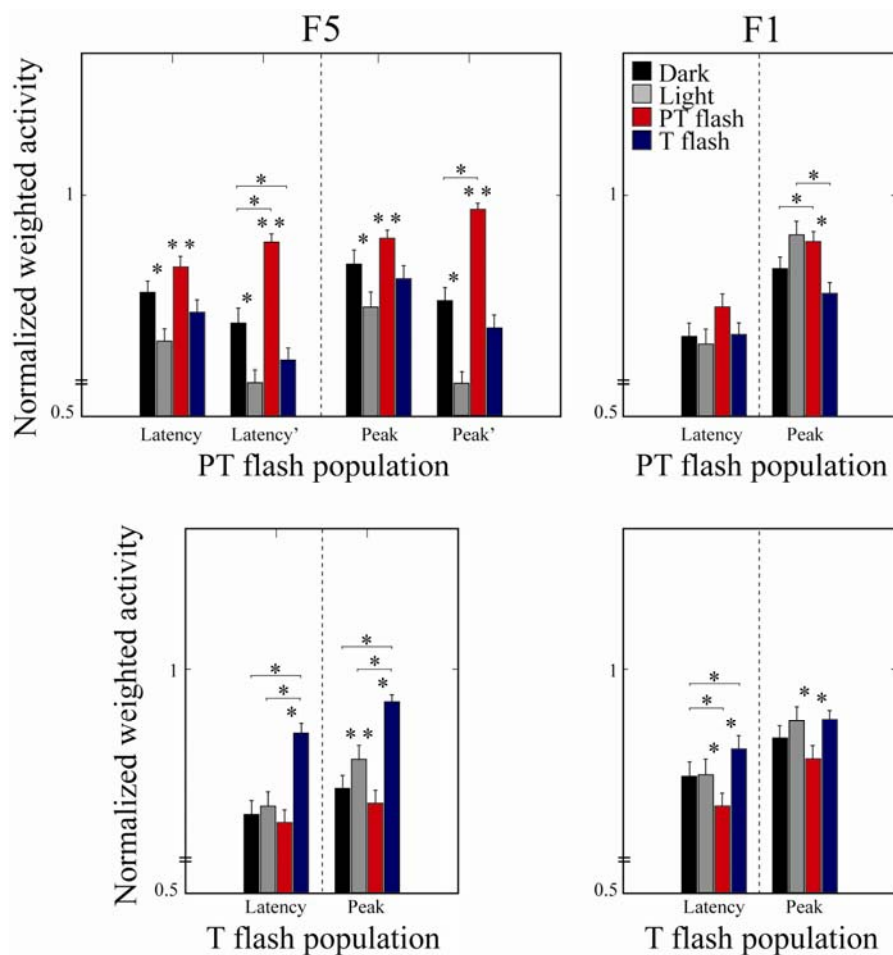


**Figure 14.** Average normalized activity of *PT* and *T flash*-responsive neurons of area F5 and F1, weighted to the time of maximum (*Peak*) and half-maximum (*Latency*) discharge displayed by all the neurons in the population in the four experimental conditions. Asterisks on top of bar plots indicate main significant differences among conditions ( $P < 0.05$ , LSD post-hoc tests, subsequent to significant one-way ANOVA *condition* main effect). *Latency'* and *Peak'*: average

discharge latency and peak of F5 *PT flash*-selective population, after that the firing temporal distribution within each condition has been leveled to that of *PT flash* condition, i.e., the most dispersed one.

shaping phase of grasping principally affected F5 recorded cells inducing a larger discharge timing variability (that can thus be considered a hallmark of the response of area F5 to *PT flash*), implied that the average peak discharge of the F5 *PT flash*-selective neurons was particularly lowered in the *PT flash* condition, where the highest data dispersion was detected. Indeed, by making the population homogeneous from the aspect of the firing temporal dispersion (i.e., by leveling the peaks distribution exhibited in each condition to the largest observed, that of *PT flash* condition), a strong *PT flash*-selectivity came out (see Fig. 14, *Latency'* and *Peak'* of the F5 *PT flash* population).

To summarize the results obtained with the last described analyses, the presence of a transient visual feedback on the own ongoing action strongly influenced the response of F5 neurons (and much more than that of F1 neurons) in the following ways: (1) the activity recorded during the delivery of the relevant light flash for a given flash-selective population was consistently higher compared to that expressed in all the other experimental conditions, including full light (on the whole, F1 flash-related firing rates did not rise above *L*-related discharge in neither population).(2) This strong flash-selectivity was evident both when comparing the absolute peak discharge reached by the neurons in each condition and the single-unit maximum activity counted against the time of peak discharge of all the neurons in a given population. (3) On average, F5 neurons, as opposed to F1 neurons, maintained their flash-selectivity well before and after arriving at the peak activity, as shown by the analysis carried out contrasting the mean firing rates during all the 500-ms grasping window of each condition. (4) F5 *PT flash*-selective neuronal group reacted to *PT flash* presentation rearranging their grasping-related response in a more distributed way (see difference between temporal peak IQR of these neurons and that measured for all the other F5 and F1 flash- and non-flash-selective populations in Tab. 5).

## DISCUSSION

The present study investigates whether ventral premotor area F5 contains visuomotor neurons which do not show any visual response associated to the observation of 3D objects (canonical neurons) or to actions performed by other individuals (mirror neurons), but rather, are sensitive to the observation of the monkey's own hand during an ongoing grasping movement. These neurons, which we proved to be present, exhibit visuomotor properties that are common to both purely motor and mirror neurons, hence allowing new speculations on the critical role of online visual information during grasping execution and on the nature/genesis of the mirror neuron visual response. Indeed, both in area F5 and in primary motor cortex (area F1) a significant percentage of neurons modulate their grasping-related activity as a function of the duration (continuous or transient) and of the instant (hand preshaping- or hand-object contact) of the hand-related visual feedback. The effects observed in these two motor areas present some important differences, suggesting a distinct functional contribution of the ventral premotor and primary motor cortices to the analysis of motor-relevant visual feedback.

*Both F5 and F1 neurons potentiate their motor activity during hand shaping in light, but F5 neurons show a faster increase of light-related responses*

By comparing the grasping-related activity of the neurons during light and dark conditions, a variety of neuronal categories could be distinguished, both in area F5 and in area F1, depending on the time course of their modulation. The main modulation was mostly due to a more prolonged activity when the monkey was grasping in dark, with respect to full vision condition. For example, while a large amount of neurons in both areas displayed overlapping pre-touch responses both in light and dark, they differentiated their response in the post-touch phase, mainly because of the contrast between the rapid firing decay observed in light and the more long-lasting activity characterizing the post-touch phase in dark. This neuronal behavior, that statistically produced a post-touch  $D > L$  effect, was rather likely related to finger posture corrections ensuing proprioceptive feedbacks from the hand-object contact in the dark, as we observed in some pilot kinematics experiments. However, being the aim of our study the detection of neurons sensitive to the vision of the own grasping hand, we concentrated on neurons that, in full light, potentiated their discharge within the period preceding the contact with the to-be-grasped object. This neuronal class was the most represented one, both in area F5 (14%) and in area F1 (13%). This result is particularly relevant since, although visual information on the own ongoing action was continuously achievable in the light condition, the activity of the majority of light-responsive recorded neurons was mainly

affected by it during hand pre-shaping and landing onto the object. We will therefore comment now in detail some properties of these pre-touch light-responsive neurons.

While the percentage of these neurons was similar in the two motor areas, both in terms of time course and in terms of light-responsiveness, an important timing difference characterized the grasping-related response of the F5 sub-population in the light condition. When the reach-to-grasp task was performed under constant online visual feedback, the latency and peak times of the discharge were significantly shorter than those observed during the execution of the same task in absence of any visual information. Conversely, F1 neurons did not show any anticipation of the grasping response recorded in light with respect to that recorded in the dark. These visuomotor neurons resemble those previously described in area AIP (Murata et al. 2000; Sakata et al. 1995) which have been suggested to play some role in encoding the pattern of hand movements during handgrip formation. The light-sensitive neurons reported in the present work, as well as the AIP “nonobject-type” neurons, did not respond to object presentation, as shown by the naturalistic testing and by the absence of any response to the mere observation of the to-be-grasped object during the formal testing.

The present findings concerning pre-touch light-dependent neuronal effects can be actually subjected to more than one specific interpretation, including, first of all, the critical influence that the online visual feedback may exert on grasping kinematics. Indeed, although the experimental apparatus was designed so as to minimize at best hand movement variations between light and dark conditions (the to-be-grasped object was made visible also in the dark), analyses carried out on the kinematic trajectories recorded during the behavioral experiment revealed some crucial, though subtle, differences between the two conditions. As reported in literature (Churchill et al. 2000; Schettino et al. 2003; Winges et al. 2003), an increase in the duration of the deceleration phase and of finger closing was found when grasping was performed in the dark. Moreover, maximum grip aperture became wider, indexing that, without vision, the monkey tended to increase the grip size safety margin for grasping the door handle successfully (Rand et al. 2007).

Consistent with these findings might be the evidence that neurons of both areas enhanced their activity just in the pre-shaping phase of the light condition. Even more relevant could be the temporal gain that pre-touch light-selective F5 neurons showed in their motor response, when the sight of the ongoing movement was allowed, compared to when it was not. This facilitation was mainly expressed as a faster rate of ramping activity of these neurons in full light, as opposed to the slow, gradually increasing firing rates during the pre-touch phase in dark. Accordingly, a 50-ms anticipation of the light over dark was measured both at the latency and peak of the grasping-related neuronal response. These F5 light-dependent timing effects, which most likely finally ended with

the strengthening of the pre-touch discharge shown by F1 neurons during light, well inversely correlate with the longer grasping approach, adopted by the monkey in the final part of reaching-grasping in absence of any visual feedback. The behavior expressed by many neurons in anticipating their motor response under full light condition (16% in F5 and 23% in F1), possibly associated with modifications of movement velocity, would well support the hypothesis that these data mostly relate to hand kinematics differences, than to observation-evoked responses. Even more generally, the finding that a higher percentage of neurons were strengthening (31%, including both areas), rather than diminishing (13%), their activity in the most critical period of the grasping movement (*pre-touch/touch* period) during light, appears to favor this interpretation. It is thus arguable that, these visuomotor cells could be present in both F5 and AIP, two strongly interconnected areas, and might form a sub-circuit specifically relevant to visual feedback-based adjustments of the handgrip during movement. More direct evidence is however required to support this hypothesis, based on systematic studies of the correlation between hand kinematics and neuronal activity.

Another possible account for the light-modulated grasping response of these neurons is that it may represent one of the many instances of the observation-evoked motor activation that is typical of mirror neurons. Indeed, it has been demonstrated that the F5 mirror visual discharge can reflect the neuron's motor selectivity at several degrees of abstraction (Nelissen et al. 2005; Gallese et al. 1996; di Pellegrino et al. 1992). Recently, also single-neuron activity in area F1 has been shown to be similar during both execution and passive observation of a familiar task. Interestingly, in the observation condition, F1 neurons fired in response to the view of a reliable surrogate of the monkey's own hand (a visual cursor projected on a screen), moving in an abstract workspace (Tkach et al. 2007).

In our study, monkeys were observing their own, as opposed to others' (co-specific or human), *active* movements. In this particular case, the action which the cells contribute to generate, perfectly matches the one potentially evoking a neuronal response in the same cells through observation. Hence, because mapped on the same active movement, the discharge elicited by observation is not easily dissociable from the one related to execution. It is thus plausible that, to be appreciated, any neuronal activation potentially induced by the vision of the own grasping movement, must be almost exclusively represented by an increase (or decrease) in light, of the activity recorded during grasping execution in dark, as in the case of the light-responsive neurons described here. However, the observation-related meaning of such a modulation cannot be distinguishable from a kinematics effect

*Both F5 and F1 neurons selectively respond to motor-relevant transient visual feedbacks, but area F5 shows a higher specificity for the type of grasping-related information they bring*

To exclude any influence of kinematics on the observation-dependent responses of the recorded neurons, two light flash conditions were introduced in our experiment. No substantial hand kinematic difference was indeed found between the two flash and the full dark conditions. Conversely, several recorded neurons displayed specific selectivity for either of the two light flash conditions, suggesting that the behavioral paradigm succeeded in revealing neuronal effects dependent on the vision of brief fragments of the own grasping action. Specifically, a large number of both F5 (48%) and F1 (43%) cells statistically showed a difference in the grasping-related activity, dependently of whether transient visual information was fed back from the handgrip configuration period or hand-object contact instant. Importantly, the latency of flash-selectivity displayed by these neuronal populations tightly reflected the point in time of flash occurrence, that is, earlier in the trial when visual feedback was given during pre-shaping, with respect to when it was delivered at the handle touch. One possible criticism may be that the found neuronal modulations rather depended on an arousal effect, time-locked to flash presentation. Our results show that this was not the case.

First, since the analysis consisted in directly contrasting the activity displayed by the same cell in the two flash conditions, all neurons showing a significant response to both flashes (that could be indicative of an arousal reaction in the monkey) were automatically not taken into consideration. Second, the flash selectivity of the neurons did not generally emerge immediately after one given flash was delivered (that would suggest the existence of a strict temporal relationship between the arrival of a transitory visual event and the onset of the neuronal response); rather, it appeared at different times around flash presentation and, in some cases, even in advance of it, meaning that neurons were not only online signaling, but also ‘expecting’, the availability of the flashed motor-relevant visual information (the experiment was performed in blocks). Moreover, particularly in area F5, cells continued conveying this information well after flash offset, denoting that this was somehow a meaningful event, rather than simply a startling stimulus, for the animal engaged in performing the grasping movement.

It is also to note that the degree of overlap between any of the light-sensitive neuronal classes and flash-selective neurons was poor in both areas, supporting the assumption that the neuronal modulations due to continuous vision of the movement were, in all probability, of a different kind with respect to those observed during brief illumination of the motor action scene. In particular, since kinematics and arousal are not to be considered important confounding variables,

the hypothesis that flash-related sensitivity represented the selective response of the neurons to the observation by the monkey of its own ongoing grasping at specific time windows (when the view of the movement was briefly made accessible), can be strongly put forward.

The fact that observation-evoked responses were recorded also in the primary motor cortex is not surprising. Significant changes in M1 cortical activity during action observation have been reported by several human studies, using different techniques (Fadiga et al. 1995; Muthukumaraswamy and Johnson 2004; Caetano et al. 2007; Cheng et al. 2007). In addition, the study mentioned above (Tkach et al. 2007) has tackled the issue of observation-related M1 activation at the single-unit level, describing neuronal discharge and local field potentials associated with the passive view of own movements.

However, the detailed analysis of the visually-modulated activity of the neurons recorded in the present research revealed that F1 flash-evoked neuronal effects differed from those found in F5 as far as some critical features are concerned. First, the level of flash selectivity, defined as the relative difference in the neuron's grasping activity between the two flash conditions, was lower in area F1 than in area F5. More relevant, the signal related to transient action observation brought by F1 neurons was in general not significantly stronger than the one they showed under continuous visual feedback conditions. In contrast, F5 neurons exhibited the maximal discharge in response to the delivery of the light flash which they were sensitive for, both at the peak and during the whole grasping time, suggesting that the visual information conveyed by the brief enlightenment of the hand movement was extremely efficient in strengthening the ongoing motor activity of these neurons.

Moreover, population analyses showed that the pattern of activation of F5 neurons was highly specific for the type of visual feedback received. In particular, the transient observation by the animal of its own movement during the handgrip configuration phase of grasping, besides augmenting considerably the motor response of the neurons, specifically increased the temporal dispersion of the discharge peaks compared to the dark condition. Conversely, the F5 population selectively active in the final period of grasping, when the monkey could briefly look at its own hand contacting the door handle, displayed a more temporally compact distribution of the neurons' firing peaks. Interestingly, a comparable firing dispersion was displayed by these populations during grasping performed in full light, whereas in the flash condition for which no selectivity was shown, the behavior of the same neurons moved towards the opposite distribution trend, approaching that taken on in absence of any visual feedback. Hence, the same visual stimulus, presented at different critical stages of the grasping action, differentially affected F5 neuronal response. This suggests that the possibility of transitorily access the view of meaningful bits of the

own ongoing action, online specifically reinforced the motor program used to execute that particular action. The computational study of motor control has provided important working principles concerning the relationship between sensory signals and motor commands. It is currently thought that the motor system is governed by two main internal processing models, also called predictors, which control the causal link between actions and their consequences (Wolpert and Ghahramani 2000). Inverse models implement the transformation from the desired consequences (i.e., the goal) of an action to the motor commands necessary to execute that action. Any form of motor pre-programming, as in the case of the present reach-to-grasp task, implicitly involves this inverse relationship. Forward models, instead, monitor the state of the current motor commands by continuously predicting the consequences of them, through sensory feedback from the periphery. Thereby, forward models can support sensorimotor control by minimizing sensory and motor noise in many ways, including integrating, invalidating or anticipating the kind of sensory inflow that constantly update predictions (Miall 2003; Bays and Wolpert 2007).

In the context of the present experiment, for instance, estimation of the state of the system could have supplemented noisy or absent visual information during grasping in full dark, or generated the appropriate adjustment signals for online grip control after, or in advance of, a visual reafference from the transient observation of the action during flash delivery. Indeed, the enhancement of motor activity in the flash-selective populations in response to the brief illumination of the grasping hand might be the result of forward predictions, intervening over the ongoing inverse sensorimotor transformation for handle grasping. In addition, the increased timing variability in the firing peaks of the neurons (measured during the brief view of the own hand before the contact with the handle) might be directly reflecting the uncertainty of handgrip estimation and thus be related to the error signal produced to fast rearrange the posture of the fingers with respect to the target. Conversely, the compacted strengthened discharge of the neurons, in response to the sight of the handle touch instant (a grasping event that is perceptually and temporally more defined than pre-shaping and hence, more easily predictable) might be indicative of a reinforcement signal, confirming the correct forward estimation of the state of the system at that point of grasping.

Taken together, these results confirm that area F5 contains visuomotor neurons which are specifically activated by the transitory observation of meaningful phases of the own grasping movement. Moreover, to a minor extent, similar effects are shown to be present also in area F1. Turning to the issue, initially addressed, of the nature of the visuomotor coupling at the basis of the mirror response, what then might be the role of these F5 neurons, showing these peculiar visuomotor properties? How can these findings be interpreted in the framework of a theory

supposed to explain the development of mirror neurons? Finally, what might be the functional interplay between F5 and F1 neurons displaying observation-evoked motor responses of the kind described by our work?

### *Interpretational issues*

It has been suggested that mirror cells, originally described in area F5, lie at a crucial interface between inverse and forward models (Iacoboni et al. 2005; Carr et al. 2003). Connections from STS to PF, and forward to mirror neurons in F5, would represent an inverse model mapping the visual description of actions onto the motor commands that are needed to execute them. The reverse projections from F5 to PF and backward to STS would instead correspond to a forward model translating the actual motor plan into a predicted sensory representation of it. This two-way model could be responsible for the activation of mirror neurons during both action execution and observation. However, though very elegant, this scheme presents some contradictory points.

First, the predictions made by forward models are, by definition, very specific, as they are to provide the motor system with helpful information to constantly control movement outcome. On the other hand, F5 observation-related mirror responses are characterized by different levels of generality. Second, forward models originally imply that estimations about the current state of the motor system mainly involve our own actions, whereas the mirror visual discharge has never been described as concerning first-person motor action observation. The hyper-MOSAIC computational model developed by Wolpert et al. (2003) takes into account the former argument, proposing that multiple paired forward/inverse models act in parallel to estimate and control motor states at different hierarchical levels of abstraction (Wolpert et al. 2003). Whereas lowest levels would imply an extremely congruent matching between executed and observed actions, the highest layers would represent the behavioral goal of actions, unbounded from the specific motor effector or kinematic details of the action. Intermediate stages would progressively receive from previous layers, coding actions at increasingly more abstract levels. How the lowest layers of this architecture can be neuronally generated is not yet well understood. The visuomotor neurons described in the present study, for the fact that they receive facilitatory inputs activated by the sight of specific phases of the own action, thus showing perfectly matched execution- and observation-related activity, could be the most appropriate elements to underpin the lowest-level forward/inverse models. In addition, given that superior layers develop from these basic models, the discharge properties of these neurons might play a critical role in the generation of the mirror visual response. This gives support to the theory which asserts that the observation of the agent's own acting effector is a fundamental step in the biological process leading to neuronal activation associated to the observation of actions performed by others (Rizzolatti and Fadiga, 1998).

The hypothesis hereby proposed is that, through the forward models normally guiding action execution, the motor system progressively extracts motor-invariant (goal-related) visual signals from the repetitive experience of performing one given action from slightly different perspectives or under conditions implying variability in the availability of the visual information relevant to the action. These visual signals that continuously change, for instance, depending on the relative position of the head and the eye with respect to the acting hand or the target object, would be generalized by virtue of the fact that they are generated by very similar motor programs, all issued to achieved the same goal. Once this generalization process, that is supposed to play a relevant part not only during development but also during learning of new motor acts in adults, is sufficiently established, it would be then gradually transferred also to actions performed by others. In so doing, the visual representation of a given observed action would gain access to the corresponding motor representation due to the coherent action description that the observer has previously acquired through the visuomotor link concerning his/her own movements. In computational terms, the more similar the observer's hyper-MOSAIC is to the actor's hyper-MOSAIC, the easier it will be to make associations between them. These associations would be at the basis of the *recognition* operations played by F5 mirror neurons and the flash-related effects found in this study, confirming that in area F5 there exist neurons that specifically respond when the agent observes his/her own movement, would represent the mechanism through which visual signals mapped on the own motor programs are progressively acquired.

Additional experiments are required to more deeply explore this complex topic, such as studying the response of these neurons when visual information about the ongoing movement is disrupted and extending the testing to F5 mirror neurons. It is interesting to note that experiments performed in artificial robotic systems aiming at simulating the development of mirror neurons through the observation of one's own hand during execution of grasping (Metta et al. 2006; Craighero et al. 2007) seem to confirm this hypothesis.

Despite that many studies, principally conducted on humans, have reported observation-evoked responses also in primary motor cortex, there is to date no evidence about the existence of mirror neurons in this area. These F1 modulations have been proposed to be not functional but simply a reflection of the strong cortico-cortical interconnections with area F5 (Fadiga et al. 1995, Kilner and Frith 2007). It is well known that F5 can influence hand muscles via its dense projections to F1 (Dum and Strick 2005). Conditioning F5 stimulation results in significant facilitation of F1 corticospinal activity and, consequently, of responses in hand motoneurons (Cerri et al. 2003; Shimazu et al. 2004; Schmidlin et al. 2008). Hence, according to this interpretation, F1

modulation during action observation could be considered as an effect of the simultaneous strong activation of area F5. An alternative hypothesis is that F1 neurons might play a specific functional role, by representing the observed actions in a different coordinate system with respect to that used by F5. In particular, it might be that whereas F5 decodes the extrinsic features of the observed action (i.e., the relative positions of the hand and of the target in space), F1 describes the intrinsic pattern of muscle activation involved in the action, similarly to what is coded by the two areas during the actual action execution (Takei et al. 2001). Specific experiments should be carried out to test both hypotheses. However, the poor action observation-related activation of F1 found in the present study, strongly suggests that it may be rather the reflective result of the highly significant modulation characterizing neuronal responses in F5.

### *Conclusions*

By this work we demonstrate that ventral premotor area F5 contains visuomotor neurons selectively strengthening their motor response during continuous or transient vision of the monkey's own grasping movement. These findings confirm that F5, as well as area AIP in the parietal lobe, is crucial for the visual control of handgrip formation during grasping. Furthermore, our results lay the ground for a visuomotor theory about the generation of mirror neurons. The specific observation-evoked motor responses described here can be thought of as the key step for transferring the meaning attributed to our own movements to actions performed by other individuals, both during development and learning of new actions.

### ACKNOWLEDGEMENTS

This work has been supported by EU Grants Mirror and RobotCub to LF

## REFERENCES

1. **Bays PM and Wolpert DM.** Computational principles of sensorimotor control that minimize uncertainty and variability. *J Physiol* 578: 387-96, 2007.
2. **Bezdek JC, Ehrlich R and Full W.** FCM: Fuzzy C-Means Algorithm. *Computers and Geoscience* 10: 191–203, 1984.
3. **Caetano G, Jousmaki V and Hari R.** Actor's and observer's primary motor cortices stabilize similarly after seen or heard motor actions. *Proc Natl Acad Sci U S A* 104: 9058-62, 2007.
4. **Carr L, Iacoboni M, Dubeau MC, Mazziotta JC and Lenzi GL.** Neural mechanisms of empathy in humans: a relay from neural systems for imitation to limbic areas. *Proc Natl Acad Sci U S A* 100: 5497-502, 2003.
5. **Cerri G, Shimazu H, Maier MA and Lemon RN.** Facilitation from ventral premotor cortex of primary motor cortex outputs to macaque hand muscles. *J Neurophysiol* 90(2): 832-842, 2003.
6. **Cheng Y, Meltzoff AN and Decety J.** Motivation modulates the activity of the human mirror-neuron system. *Cereb Cortex* 17: 1979-86, 2007.
7. **Churchill A, Hopkins B, Ronnqvist L and Vogt S.** Vision of the hand and environmental context in human prehension. *Exp Brain Res* 134: 81-9, 2000.
8. **Craighero L, Metta G, Sandini G and Fadiga L.** The mirror-neurons system: data and models. *Prog Brain Res* 164: 39-59, 2007.
9. **di Pellegrino G, Fadiga L, Fogassi L, Gallese V and Rizzolatti G.** Understanding motor events: a neurophysiological study. *Exp Brain Res* 91: 176-80, 1992.
10. **Dum RP and Strick PL.** Frontal lobe inputs to the digit representations of the motor areas on the lateral surface of the hemisphere. *J Neurosci* 25: 1375-86, 2005.
11. **Fadiga L, Fogassi L, Pavesi G and Rizzolatti G.** Motor facilitation during action observation: a magnetic stimulation study. *J Neurophysiol* 73: 2608-11, 1995.
12. **Fogassi L, Ferrari PF, Gesierich B, Rozzi S, Chersi F and Rizzolatti G.** Parietal lobe: from

action organization to intention understanding. *Science* 308: 662-7, 2005.

13. **Fogassi L, Gallese V, Buccino G, Craighero L, Fadiga L and Rizzolatti G.** Cortical mechanism for the visual guidance of hand grasping movements in the monkey: A reversible inactivation study. *Brain* 124: 571-86, 2001.
14. **Fogassi L and Luppino G.** Motor functions of the parietal lobe. *Curr Opin Neurobiol* 15: 626-31, 2005.
15. **Gallese V, Fadiga L, Fogassi L and Rizzolatti G.** Action recognition in the premotor cortex. *Brain* 119 ( Pt 2): 593-609, 1996.
16. **Gawne TJ, Kjaer TW and Richmond BJ.** Latency: another potential code for feature binding in striate cortex. *J Neurophysiol* 76: 1356-60, 1996.
17. **Gentilucci M, Toni I, Chieffi S and Pavesi G.** The role of proprioception in the control of prehension movements: a kinematic study in a peripherally deafferented patient and in normal subjects. *Exp Brain Res* 99: 483-500, 1994.
18. **Iacoboni M, Molnar-Szakacs I, Gallese V, Buccino G, Mazziotta JC and Rizzolatti G.** Grasping the intentions of others with one's own mirror neuron system. *PLoS Biol* 3: e79, 2005.
19. **Jackson SR, Jackson GM and Rosicky J.** Are non-relevant objects represented in working memory? The effect of non-target objects on reach and grasp kinematics. *Exp Brain Res* 102: 519-30, 1995.
20. **Jakobson LS and Goodale MA.** Factors affecting higher-order movement planning: a kinematic analysis of human prehension. *Exp Brain Res* 86: 199-208, 1991.
21. **Jeannerod M.** The formation of finger grip during prehension. A cortically mediated visuomotor pattern. *Behav Brain Res* 19: 99-116, 1986.
22. **Jeannerod M, Arbib MA, Rizzolatti G and Sakata H.** Grasping objects: the cortical mechanisms of visuomotor transformation. *Trends Neurosci* 18: 314-20, 1995.
23. **Takei S, Hoffman DS and Strick PL.** Direction of action is represented in the ventral premotor cortex. *Nat Neurosci* 4: 1020-5, 2001.

24. **Kilner JM and Frith CD.** A possible role for primary motor cortex during action observation. *Proc Natl Acad Sci U S A* 104: 8683-4, 2007.
25. **Lewicki MS.** A review of methods for spike sorting: the detection and classification of neural action potentials. *Network* 9: R53-78, 1998.
26. **Liu Y and Rouiller EM.** Mechanisms of recovery of dexterity following unilateral lesion of the sensorimotor cortex in adult monkeys. *Exp Brain Res* 128: 149-59, 1999.
27. **Matelli M, Camarda R, Glickstein M and Rizzolatti G.** Afferent and efferent projections of the inferior area 6 in the macaque monkey. *J Comp Neurol* 251: 281-98, 1986.
28. **Metz CE.** Basic principles of ROC analysis. *Semin Nucl Med* 8: 283-98, 1978.
29. **Metta G, Sandini G, Natale L, Craighero L and Fadiga L.** Understanding mirror neurons: a bio-robotic approach. *Interaction Studies* 7(2): 197-232, 2006.
30. **Miall RC.** Connecting mirror neurons and forward models. *Neuroreport* 14: 2135-7, 2003.
31. **Murata A, Fadiga L, Fogassi L, Gallese V, Raos V and Rizzolatti G.** Object representation in the ventral premotor cortex (area F5) of the monkey. *J Neurophysiol* 78: 2226-30, 1997.
32. **Murata A, Gallese V, Kaseda M and Sakata H.** Parietal neurons related to memory-guided hand manipulation. *J Neurophysiol* 75: 2180-6, 1996.
33. **Murata A, Gallese V, Luppino G, Kaseda M and Sakata H.** Selectivity for the shape, size, and orientation of objects for grasping in neurons of monkey parietal area AIP. *J Neurophysiol* 83: 2580-601, 2000.
34. **Muthukumaraswamy SD and Johnson BW.** Primary motor cortex activation during action observation revealed by wavelet analysis of the EEG. *Clin Neurophysiol* 115: 1760-6, 2004.
35. **Nelissen K, Luppino G, Vanduffel W, Rizzolatti G and Orban GA.** Observing others: multiple action representation in the frontal lobe. *Science* 310: 332-6, 2005.
36. **Perrett DI, Harries MH, Bevan R, Thomas S, Benson PJ, Mistlin AJ, Chitty AJ, Hietanen JK and Ortega JE.** Frameworks of analysis for the neural representation of animate objects and actions. *J Exp Biol* 146: 87-113, 1989.
37. **Petrides M and Pandya DN.** Projections to the frontal cortex from the posterior parietal

region in the rhesus monkey. *J Comp Neurol* 228: 105-16, 1984.

38. **Rand MK, Lemay M, Squire LM, Shimansky YP and Stelmach GE.** Role of vision in aperture closure control during reach-to-grasp movements. *Exp Brain Res* 181: 447-60, 2007.
39. **Raos V, Umilta MA, Gallese V and Fogassi L.** Functional properties of grasping-related neurons in the dorsal premotor area F2 of the macaque monkey. *J Neurophysiol* 92: 1990-2002, 2004.
40. **Raos V, Umilta MA, Murata A, Fogassi L and Gallese V.** Functional properties of grasping-related neurons in the ventral premotor area F5 of the macaque monkey. *J Neurophysiol* 95: 709-29, 2006.
41. **Rizzolatti G, Camarda R, Fogassi L, Gentilucci M, Luppino G and Matelli M.** Functional organization of inferior area 6 in the macaque monkey. II. Area F5 and the control of distal movements. *Exp Brain Res* 71: 491-507, 1988.
42. **Rizzolatti G and Fadiga L.** Grasping objects and grasping action meanings: the dual role of monkey rostroventral premotor cortex (area F5). *Novartis Found Symp* 218: 81-95; discussion 95-103, 1998.
43. **Rizzolatti G, Fadiga L, Gallese V and Fogassi L.** Premotor cortex and the recognition of motor actions. *Brain Res Cogn Brain Res* 3: 131-41, 1996.
44. **Rizzolatti G, Gentilucci M, Camarda RM, Gallese V, Luppino G, Matelli M and Fogassi L.** Neurons related to reaching-grasping arm movements in the rostral part of area 6 (area 6a beta). *Exp Brain Res* 82: 337-50, 1990.
45. **Rizzolatti G and Luppino G.** The cortical motor system. *Neuron* 31: 889-901, 2001.
46. **Sakata H, Taira M, Murata A and Mine S.** Neural mechanisms of visual guidance of hand action in the parietal cortex of the monkey. *Cereb Cortex* 5: 429-38, 1995.
47. **Schettino LF, Adamovich SV and Poizner H.** Effects of object shape and visual feedback on hand configuration during grasping. *Exp Brain Res* 151: 158-66, 2003.
48. **Schmidlin E, Brochier T, Maier MA, Kirkwood PA and Lemon RN.** Pronounced reduction of digit motor responses evoked from macaque ventral premotor cortex after reversible inactivation of the primary motor cortex hand area. *J Neurosci* 28(22): 5772-83,

2008.

49. **Schmitzer-Torbert N, Jackson J, Henze D, Harris K and Redish AD.** Quantitative measures of cluster quality for use in extracellular recordings. *Neuroscience* 131: 1-11, 2005.
50. **Shimazu H, Maier MA, Cerri G, Kirkwood PA and Lemon RN.** Macaque ventral premotor cortex exerts powerful facilitation of motor cortex outputs to upper limb motoneurons. *J Neurosci* 24: 1200-11, 2004.
51. **Szabo J and Cowan WM.** A stereotaxic atlas of the brain of the cynomolgus monkey (*Macaca fascicularis*). *J Comp Neurol* 222: 265-300, 1984.
52. **Taira M, Mine S, Georgopoulos AP, Murata A and Sakata H.** Parietal cortex neurons of the monkey related to the visual guidance of hand movement. *Exp Brain Res* 83: 29-36, 1990.
53. **Tkach D, Reimer J and Hatsopoulos NG.** Congruent activity during action and action observation in motor cortex. *J Neurosci* 27: 13241-50, 2007.
54. **Umiltà MA, Brochier T, Spinks RL and Lemon RN.** Simultaneous recording of macaque premotor and primary motor cortex neuronal populations reveals different functional contributions to visuomotor grasp. *J Neurophysiol* 98: 488-501, 2007.
55. **Umiltà MA, Kohler E, Gallese V, Fogassi L, Fadiga L, Keysers C and Rizzolatti G.** I know what you are doing. a neurophysiological study. *Neuron* 31: 155-65, 2001.
56. **Winges SA, Weber DJ and Santello M.** The role of vision on hand preshaping during reach to grasp. *Exp Brain Res* 152: 489-98, 2003.
57. **Wolpert DM, Doya K and Kawato M.** A unifying computational framework for motor control and social interaction. *Philos Trans R Soc Lond B Biol Sci* 358: 593-602, 2003.
58. **Wolpert DM and Ghahramani Z.** Computational principles of movement neuroscience. *Nat Neurosci* 3 Suppl: 1212-7, 2000.